

TG-806

JANUARY 1966


*Technical Memorandum*

**EVOLUTION OF A PLASMA  
PUFF IN A LONGITUDINAL  
MAGNETIC FIELD**

by S. J. MOSS

THE JOHNS HOPKINS UNIVERSITY • APPLIED PHYSICS LABORATORY  
8621 Georgia Avenue, Silver Spring, Maryland 20910

Operating under Contract NOw 62-0604-c, Bureau of Naval Weapons, Department of the Navy



Distribution of this document is unlimited.

## ABSTRACT

The hydromagnetic model of the evolution of a plasma puff in a  $B_z$  field described by Waelbroeck has been used to analyze the characteristics of the plasma produced by the APL conical pinch gun. The analysis is based on fitting the signals induced in single turn magnetic pick-up loops by the passing plasma. In the cases studied good fits to the signals have been achieved and the characteristic parameters of the plasma found. This analysis applied to plasma generated by the APL theta-pinch gun has not been successful. In the two cases studied, the lack of good fits is attributed to the presence of a sizeable amount of trapped field in the puff which is present along the entire flight path through the  $B_z$  field.

PRECEDING PAGE BLANK NOT FILMED.

## TABLE OF CONTENTS

I.	Introduction . . . . .	1
II.	Theory . . . . .	3
III.	Magnetic Loop Signals Induced by the Plasma .	16
IV.	Determination of Parameters from Magnetic Signals . . . . .	21
V.	Analysis . . . . .	26
VI.	Computer Analysis . . . . .	29
VII.	Results . . . . .	41
VIII.	Discussion . . . . .	43
Appendices		
I.	Solution of Equation 10b . . . . .	44
II.	Solution of Equation 12 . . . . .	46
III.	Solution of Equation 22 . . . . .	47
IV.	The Compensated Magnetic Loops . . . . .	50
V.	Computer Listings . . . . .	52
	References . . . . .	62

PRECEDING PAGE BLANK NOT FILMED.

## LIST OF ILLUSTRATIONS

<u>Figure</u>		<u>Page</u>
1	Experimental Arrangement . . .	12
2	Magnetic Loop and Field Geometry . .	17
3	Domain of Allowable Values of ( $f^*$ , $\Lambda^*$ ) . .	24
4	Typical Magnetic Loop Signals . . .	33
5	Comparison of Magnetic Loop Signals with Analysis (points), Condition I . .	35
6	Comparison of Magnetic Loop Signals with Analysis (points), Condition II . .	38

PRECEDING PAGE BLANK NOT FILMED.

## I. INTRODUCTION

This report is an elaboration of the work conducted by the fusion research group (Ref. 1) at Fontenay-aux-Roses during the period 1960-1964 concerning the analysis of plasma flow through a longitudinal magnetic field. This report includes a more comprehensive discussion of the model which was presented by the French scientists as well as the analysis of plasma flow made by the Plasma Dynamics Group at the Applied Physics Laboratory. The computer analysis, developed at the Laboratory, is also discussed in some detail.

The model describes the plasma by means of hydromagnetic equations with some simplifying assumptions. It is shown that the model is able to extract the gross features of the plasma (such as temperature, density, center of mass and local velocity) from magnetic loop signals induced by the plasma while passing along the field. The hydromagnetic description makes it immediately obvious that this analysis is applicable to a rather restricted class of plasmoids. Nevertheless, in the original work (Ref. 1) it was found that whenever the model could be made to fit the experimental data, the theoretical model predictions and those of more direct diagnostic techniques were in excellent agreement. Therefore, this theory is considered very useful, albeit to a restricted family of plasmas.

Both the French workers and those at APL analyzed plasmas which were produced by a conical pinch gun. The gun coils used in both cases were, in most respects, identical. However, whereas the French gun was powered by a 10  $\mu$ f capacitor bank, the APL gun used three 14- $\mu$ f capacitors and had a nominal frequency of 80 kc. The maximum allowable charging voltage was limited to 14-kv by the current capacity of the ignitron switches.

It is hoped that this analysis can be extended to the diagnosis of a plasma puff in a multipole magnetic field. The work discussed here and the investigation of this more complicated magnetic configuration are being supported by the National Aeronautics and Space Administration, Physics of Fluids Branch.

## II. THEORY

The evolution of a plasma puff as it passes through a longitudinal magnetic field has been described by Waelbroeck et al in Ref. 1. The hydro-magnetic equations have been used with the following assumptions:

1. The longitudinal guide field does not impede axial motion of the plasma, but it does eliminate radial diffusion. The density is sufficiently low that diffusion across the magnetic field is not appreciable during the time of interest.

2. At any time,  $t$ , and for a given axial position, the plasma characteristics are independent of the radial coordinate,  $r$ , up to the boundary of the plasma,  $r_p$ .

3. The collision frequency is sufficiently high that the perpendicular and parallel temperatures (with respect to the direction of the guide field) are equal at every point, i. e.,  $T_{e\parallel} = T_{e\perp}$ ,  $T_{i\parallel} = T_{i\perp}$ .

4. The plasma is electrically neutral ( $n_i \zeta = n_e$ ) and each fluid element, either electron and ion gas, has the same average velocity ( $\bar{V}_e = \bar{V}_i$ ), where  $n_i$ ,  $n_e$  and  $\zeta$  are the ion density, electron density and ionic charge, respectively. This assumption eliminates any longitudinal current.

5. The magnetic pressure and plasma pressure are in equilibrium at every instant.

6. At every instant, the linear density of the ions in the plasma with respect to the center of mass of the puff is Gaussian, i. e.,

$$N_l = \frac{N_i}{\sqrt{\pi} \lambda(t)} \exp - \left[ \frac{z}{\lambda(t)} \right]^2, \quad (1)$$

where  $N_i$  is the total number of ions in the puff,  $z$  is the coordinate relative to the center of mass of the puff and  $\lambda(t)$  is the characteristic width of the Gaussian distribution.

The momentum transfer equation with scalar pressure (see Ref. 2) can be written in the following form:

$$\rho \frac{\partial \vec{V}}{\partial t} - \vec{\nabla} \vec{V} \cdot (\rho \vec{V}) + \vec{\nabla} (n_i m_i \vec{V}_i \vec{V}_i) + \vec{\nabla} (n_e m_e \vec{V}_e \vec{V}_e) = \sigma \vec{E} + (\vec{J} \times \vec{B}) - \vec{\nabla} p - \rho \vec{\nabla} \phi, \quad (2)$$

where  $V_i$  and  $V_e$  = the ion and electron velocities with respect to the center of mass,

$m_i$  and  $m_e$  are the corresponding masses of these particles.

$$\sigma = (n_i e - n_e) e \quad (\text{charge density}) \quad (3a)$$

$$\rho = n_i m_i + n_e m_e \quad (\text{mass density}) \quad (3b)$$

$$\vec{V} = \frac{1}{\rho} (n_i m_i \vec{V}_i + n_e m_e \vec{V}_e) \quad (\text{macroscopic velocity}) \quad (3c)$$

$$\vec{J} = (n_i e V_i - n_e V_e) e \quad (\text{current density}) \quad (3d)$$

$p$  = the total scalar pressure (electron plus ion pressure)

$\vec{B}$  = the applied magnetic field, and

$\phi$  = the gravitational potential.

Neglecting the gravitational term and the electron mass compared to the ion mass, Eq. 2 becomes:

$$n_i m_i \frac{\partial \vec{V}_i}{\partial t} - \vec{V}_i \vec{\nabla} \cdot (n_i m_i \vec{V}_i) + \vec{\nabla} \cdot (n_i m_i \vec{V}_i \vec{V}_i) = \sigma \vec{E} + (\vec{J} \times \vec{B}) - \vec{\nabla} p. \quad (4)$$

But,

$$\vec{\nabla} (n_i m_i \vec{V}_i \vec{V}_i) = n_i m_i \vec{V}_i \cdot \vec{\nabla} \vec{V}_i + \vec{V}_i \vec{\nabla} (n_i m_i \vec{V}_i). \quad (5)$$



Using Eq. 5 and assumption 4, Eq. 4 becomes

$$m_i \frac{\partial \vec{V}_i}{\partial t} + m_i \vec{V}_i \cdot \nabla \vec{V}_i = - \frac{1}{n_i} \nabla p + (\vec{J} \times \vec{B}). \quad (6)$$

This is the equation of motion which will be used to describe the plasma.

In a one-dimensional flow problem, Eq. 6 reduces to

$$n_i m_i \frac{\partial \vec{V}_i}{\partial t} + n_i m_i \vec{V}_i \frac{\partial \vec{V}_i}{\partial z} + \frac{\partial p}{\partial z} = 0 \quad (7)$$

It is interesting to note that this equation describes the flow of a simple fluid with the thermal energy density,  $3/2 n_i k (T_e + T_i)$ , under the force  $-\frac{1}{n_i} \nabla p$  (where  $k$  is the Boltzmann constant).

The basic parameters are defined as follows:

1.  $\lambda_0$  and  $\lambda(t)$  are the characteristic widths of the puff along the axis at  $t = 0$  and at any time  $t$ , respectively. It should be noted that  $\lambda(t)$  is a function of time only. Time zero is defined as the time at which the puff begins to expand axially and is not necessarily the time of ejection from the gun.
2.  $v_0$  is the velocity of the center of mass of the puff.  $v(Z, t)$  is the velocity of any element of the fluid at a distance,  $Z$  centimeters, from the initial position of the center of mass and at a time,  $t$  seconds, after the expansion begins.
3.  $B_0$  is the guide-field intensity.
4.  $r_3$  is the radius of the flux conserver on which the solenoid is wound.
5.  $r_p$  is the radius of the flux tube in which the plasma travels and will vary with position and time.  $r_0$  is the radius of this flux tube when the plasma is not present. The total magnetic flux inside the flux conserver is constant.

The volume density of the ions, expressed in a form similar to Eq. 1, is given by

$$n_i = \frac{N_A}{\sqrt{\pi} \lambda(t)} \exp - \left[ \frac{z}{\lambda} \right]^2 \quad (8)$$

where  $N_A$  is the number of ions in an infinitely long cylinder of unit cross-sectional area. Using this expression in the equation of continuity,

$$\frac{\partial n_i}{\partial t} + \frac{\partial}{\partial z} (n_i V_i) = 0, \quad (9)$$

one obtains

$$\frac{\partial n_i}{\partial t} = n_i \left[ \frac{2z^2}{\lambda^3} - \frac{1}{\lambda} \right] \lambda'; \quad \lambda' = \frac{d\lambda}{dt}, \quad (10a)$$

and

$$n_i V_i = - \lambda' \int \left[ \frac{2z^2 n_i}{\lambda^3} - \frac{n_i}{\lambda} \right] dz. \quad (10b)$$

It can be shown (see Appendix I) that the solution for this velocity relative to the center of mass which is anti-symmetric for  $\pm z$  is

$$V_i = \frac{z \lambda'}{\lambda} \quad (11)$$

The equation of motion, Eq. 7, now becomes

$$\frac{\partial p}{\partial z} + \frac{n_i m_i z \lambda''}{\lambda} = 0, \quad (12)$$

which has the solution (see Appendix II) expressed by

$$p = \frac{1}{2} n_i m_i \lambda \lambda'' \quad (13)$$

Since it has been assumed that  $T_{||} = T_{\perp}$  for each component gas, the ideal gas law is applicable, i. e.,

$$p = n_i k T_i + n_e k T_e = n_i k (T_i + T_e), \quad (14)$$

and thus

$$k (T_e + T_i) = \frac{1}{2} m_i \lambda \lambda''. \quad (15)$$

From this it may be seen that the temperature is a function of time only and therefore is uniform in space. This implies, for a Gaussian density distribution and a plasma-field equilibrium at each instant, that the plasma radius,  $r_p$ , varies with  $z$ .

The total energy of the plasma puff will be considered to exclude the effect of external forces. This total energy is composed of the thermal energy of the ions and the electrons plus the kinetic energy of the ions' axial motion. The kinetic energy of the axial motion of electrons is negligible since  $\vec{V}_i = \vec{V}_e$  and  $m_i \gg m_e$ . The energy,  $W$ , is defined as

$$W = \frac{3}{2} \int_{-\infty}^{\infty} \int_0^{r_p} n_i k (T_e + T_i) 2 \pi r dr dz + \frac{1}{2} \int_{-\infty}^{\infty} \int_0^{r_p} n_i m_i V_i^2 2 \pi r dr dz. \quad (16)$$

The ideal solution would be to integrate Eq. 16 over the radius of the plasma and thus calculate the energy per unit area. Equating the pressure, Eq. 14, to the energy density would then give a useful relationship. Unfortunately,  $r$  is not known as a function of  $z$  and thus the integral cannot be evaluated exactly. However, if only an undefined low  $\beta$  plasma is considered, the plasma radius can be said to vary slowly with  $z$ . Equation 16 may now be written as

$$\frac{W}{\pi r_p^2} = \frac{3}{2} \int_{-\infty}^{\infty} n_i k (T_e + T_i) dz + \frac{1}{2} \int_{-\infty}^{\infty} n_i m_i V_i^2 dz. \quad (17)$$

Combining Eqs. 11, 15, and 17 and integrating the result yields

$$\frac{W}{\pi r_p^2} = \frac{3}{4} m_i N_A \lambda \lambda'' + \frac{1}{4} m_i N_A \lambda'^2. \quad (18)$$

Within the limits of the restricted  $\beta$ , this expression is equal to a constant which can be evaluated at time zero, i. e.,

$$\text{at } t = 0, \lambda = \lambda_0 \text{ and } \lambda' = 0,$$

and hence

$$\frac{W}{\pi r_p^2} = \frac{3}{2} N_A k (T_e + T_i)_0.$$

The approximation of low  $\beta$  must be examined more carefully. The  $\beta$  of the plasma is defined in the usual way as

$$\beta = p (B_e^2 / 2\mu_0)^{-1} = 1 - \left[ \frac{B}{B'} \right]^2 \approx 1 - \left[ \frac{B}{B_0} \right]^2, \quad (19)$$

where  $B$  is the field inside the plasma boundary and  $B'$  is the field on the vacuum side of this boundary. The external field,  $B'$ , is approximately equal to the unperturbed field,  $B_0$ , as long as the plasma radius is small compared with the radius of the solenoid (this is usually the case). Then, from the conservation of flux,

$$\pi r_p^2 B = \pi r_0^2 B_0,$$

and Eq. 19 takes the form

$$\beta = 1 - \left[ \frac{r_0}{r_p} \right]^4$$

or

$$\frac{r_0}{r_p} = (1 - \beta)^{\frac{1}{4}}. \quad (20)$$

When  $\beta = 0.6$ , the ratio of the flux tube radius to the plasma radius is about 0.8. Thus even for relatively high  $\beta$  plasma, the plasma radius changes slowly with  $z$  and the approximation used in Eq. 17 is a fairly good one.

The following reduced variables are now defined:

$$\Lambda = \frac{\lambda(t)}{\lambda_0}, \quad (21a)$$

and

$$r = \frac{t}{\xi},$$

where

$$\xi = \left[ \frac{m_i \lambda_0^2}{6k (T_e + T_i)_0} \right]^{\frac{1}{2}}. \quad (21b)$$

Differentiating Eq. 21a yields

$$\lambda' = \frac{d\lambda}{dt} = \lambda_o \frac{d\Lambda}{d\tau} \frac{d\tau}{dt} = \frac{\lambda_o}{\xi} \frac{d\Lambda}{d\tau} ,$$

and

$$\lambda'' = \frac{d^2\lambda}{dt^2} = \frac{\lambda_o}{\xi^2} \frac{d^2\Lambda}{d\tau^2} .$$

Equation 18 can now be written in terms of these variables as

$$\frac{3}{4} N_A m_i \Lambda \frac{\lambda_o^2}{\xi^2} \frac{d^2\Lambda}{d\tau^2} + \frac{1}{4} N_A m_i \frac{\lambda_o^2}{\xi^2} \left[ \frac{d\Lambda}{d\tau} \right]^2 = \frac{3}{2} N_A k (T_e + T_i)_o ,$$

which reduces to

$$3 \Lambda \frac{d^2\Lambda}{d\tau^2} + \left[ \frac{d\Lambda}{d\tau} \right]^2 = 1 . \quad (22)$$

This differential equation expresses the conservation of energy. The solution of this non-linear differential equation, as given in Appendix III, is

$$\tau = (\Lambda^{\frac{2}{3}} + 2) (\Lambda^{\frac{2}{3}} - 1)^{\frac{1}{2}} , \quad (23)$$

and

$$\frac{d\Lambda}{d\tau} = (1 - \Lambda^{-\frac{2}{3}})^{\frac{1}{2}} . \quad (24)$$

These equations combine with Eq. 15 to yield

$$k (T_e + T_i) = 3 k (T_e + T_i)_o \Lambda \frac{d^2\Lambda}{d\tau^2} ,$$

and thus

$$\frac{(T_e + T_i)}{(T_e + T_i)_o} = \frac{1}{\Lambda^{\frac{2}{3}}} = \left[ \frac{\lambda_o}{\lambda(t)} \right]^{\frac{2}{3}} . \quad (25)$$

The information which has been gathered thus far about the plasma is not in a useful form. These equations must be expressed in the laboratory coordinate system rather than in the center-of-mass system and they must be related to experimentally measurable quantities.

Beginning with the coordinate transformation, it can be seen that the laboratory axial position (measured from the center of the gun coil to any location,  $z$ , relative to the center of mass of the puff, see Fig. 1) is given by

$$Z = z + v_0 t_0 + v_0 t = z + Z_0 + v_0 t, \quad (26)$$

where  $Z_0 = v_0 t_0$  is the laboratory position at which the puff begins to expand. Thus,

$$z = Z - Z_0 - v_0 t. \quad (27)$$

The fact that expansion does not take place immediately can probably be accounted for as follows:

1. Ions formed downstream are ejected earlier than other ions but with a lower velocity. Thus, the ions tend to bunch initially.
2. Since the model does not include the possibility of a trapped field which inhibits expansions, the analysis is applicable only after this field has been dissipated.

Some of the expressions derived earlier may now be rewritten as

$$\frac{z}{\lambda(t)} = \frac{Z - Z_0 - v_0 t}{\lambda(t)} = \frac{\frac{Z - Z_0}{\lambda_0} - \frac{v_0 t}{\lambda_0}}{\Lambda} = \frac{\frac{Z - Z_0}{\lambda_0} - \frac{v_0 \tau \xi}{\lambda_0}}{\Lambda}. \quad (28)$$

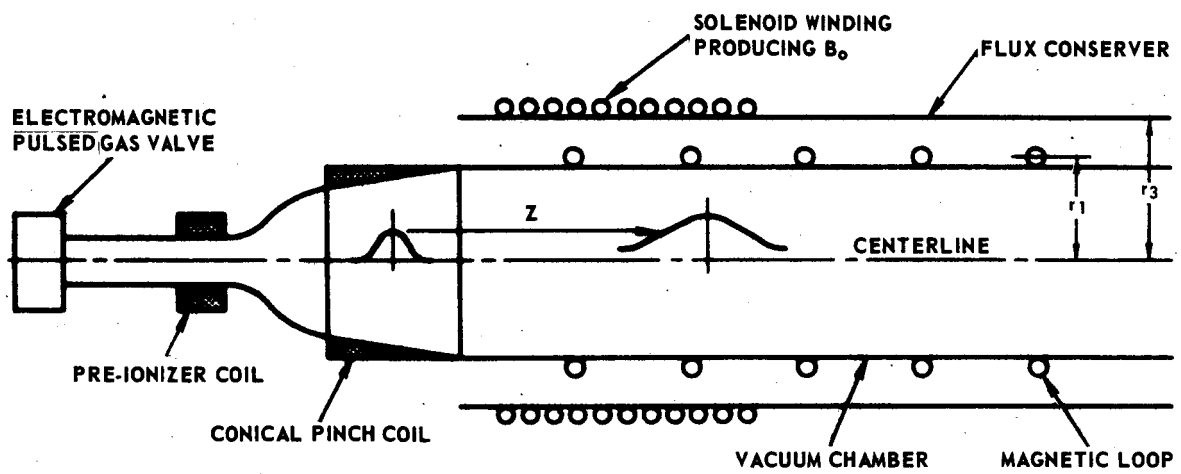


Fig. 1 Experimental Arrangement



Defining

$$\alpha = \frac{\xi v_o}{\lambda_o} = \left[ \frac{m_i v_o^2}{6k(T_e + T_i)} \right]^{\frac{1}{2}}, \quad (29)$$

and

$$Z' = \frac{Z - Z_o}{\lambda_o}, \quad (30)$$

Eqs. 1 and 8 become, respectively,

$$N_l = \frac{N_i}{\sqrt{\pi} \lambda_o \Lambda} \exp - \left[ \frac{Z' - \alpha \tau}{\Lambda} \right]^2, \quad (31)$$

and

$$n_i = \frac{N_A}{\sqrt{\pi} \lambda_o \Lambda} \exp - \left[ \frac{Z' - \alpha \tau}{\Lambda} \right]^2. \quad (32)$$

The transverse energy per unit length of the plasma,  $W_{l\perp}$  is

$$W_{l\perp} = N_l k (T_e + T_i) = \frac{N_i k (T_e + T_i)}{\sqrt{\pi} \lambda_o \Lambda} \exp - \left[ \frac{Z' - \alpha \tau}{\Lambda} \right]^2. \quad (33)$$

But from Eq. 25 we have

$$(T_e + T_i) = \frac{(T_e + T_i)_o}{\Lambda^{\frac{2}{3}}},$$

and thus

$$W_{l\perp} = \frac{N_i m_i v_o}{6 \sqrt{\pi} \alpha \xi} f(\Lambda, \alpha, Z'), \quad (34)$$

where

$$f(\Lambda, \alpha, Z') = \Lambda^{-5/3} \exp - \left[ \frac{Z' - \alpha \tau}{\Lambda} \right]^2. \quad (35)$$

$\beta$  may now be expressed in terms of the linear transverse energy density. Since

$$\beta = \frac{2 \mu_o p}{B_o^2} = \frac{2 \pi r_p^2 \mu_o p}{\pi r_p^2 B_o^2} ,$$

and

$$p \pi r_p^2 = W_{\ell \perp} ,$$

then

$$\beta = \frac{2 \mu_o W_{\ell \perp}}{\pi r_p^2 B_o^2} = 2A \left[ \frac{r_o}{r_p} \right]^2 = 2A \left[ \frac{B}{B_o} \right] , \quad (36)$$

where A is defined as

$$A = \frac{\mu_o W_{\ell \perp}}{\pi r_o^2 B_o^2} = \frac{\mu_o N_i m_i v_o}{6 \pi^{3/2} \alpha \xi r_o^2 B_o^2} f(\Lambda, \alpha, Z') . \quad (37)$$

But  $\beta$  has been defined by

$$\beta = 1 - \left[ \frac{B}{B_o} \right]^2 , \quad (38)$$

and

$$2A \left[ \frac{B}{B_o} \right] = 1 - \left[ \frac{B}{B_o} \right]^2 . \quad (39)$$

From this it follows immediately that

$$\frac{B}{B_o} = \left[ \frac{r_o}{r_p} \right]^2 = \sqrt{A^2 + 1} - A . \quad (40)$$

From Eq. (32) the ion density may now be written as

$$n_i(Z', \tau) = \frac{N_i}{\pi r_p^2} = \frac{N_i}{\pi^{3/2} \lambda_o r_o^2 \Lambda} \exp - \left[ \frac{Z' - \alpha \tau}{\Lambda} \right]^2,$$

or

$$n_i(Z', \tau) = \frac{N_i}{\pi^{3/2} \lambda_o r_o^2} \frac{(\sqrt{A^2 + 1} - A) \exp - \left[ \frac{Z' - \alpha \tau}{\Lambda} \right]^2}{\Lambda}. \quad (41)$$

The local plasma velocity,  $v(Z', \tau)$  may also be obtained. It is the sum of the center-of-mass velocity and the ion velocity (with respect to the center of mass), i. e.,  $v(Z', \tau) = V_o + V_i = V_o + \frac{Z\lambda'}{\lambda}$ , which becomes

$$v(Z', \tau) = \frac{\lambda_o}{\xi} \left[ \alpha + \left( \frac{Z' - \alpha \tau}{\Lambda} \right) \frac{d\Lambda}{d\tau} \right], \quad (42a)$$

or

$$v(Z', \tau) = \frac{\lambda_o}{\xi} \left[ \alpha + \left( \frac{Z' - \alpha \tau}{\Lambda} \right) \left( 1 - \Lambda^{-2/3} \right)^{1/2} \right]. \quad (42b)$$

It can be seen from the above discussion that the evolution of the plasma puff can be described by six parameters:  $v_o$ ,  $(T_e + T_i)_o$ ,  $Z_o$ ,  $\lambda_o$ ,  $N_i$  and  $r_o$  or, equivalently, by  $\alpha$ ,  $\xi$ ,  $Z_o$ ,  $\lambda_o$ ,  $\frac{A}{f(\Lambda)}$  and  $r_o$ . The remainder of this report will discuss means of finding these parameters from an analysis of magnetic loop signals.

### III. MAGNETIC LOOP SIGNALS INDUCED BY THE PLASMA

The work of Waelbroeck et al (Ref. 1) differs slightly from the APL work in that the French investigators used a special type of magnetic probe, called a compensated magnetic loop, while simple single-turn pick-up loops have been used at APL. The compensated loops are discussed in Appendix IV and, as can be seen, have some definite advantages over the system used here. However, since one of the primary purposes of the present work is to extend this analysis to the multipole magnetic configuration where only simple loops can be used, the convenience of the compensated loops is sacrificed.

Figure 2 is a schematic representation of the drift field and a simple magnetic loop. The period of the field is very long compared to the transit time of the plasma, and the field is spatially uniform inside the flux conserver. The plasma effectively excludes part of the field from the volume which it otherwise occupies. In the presence of the flux conserver, this excluded flux is distributed over the volume between  $r_p$  and the conserver radius,  $r_3$ . For a plasma whose length is long compared to  $r_3$ , this distribution can be considered uniform.

Assume  $B_0$  is the drift field strength in the absence of plasma,

$-B_p$  is the field generated by currents internal to the plasma,  
and

$B_e$  is the increase in the field strength external to the plasma  
caused by the presence of the plasma.

With the previous assumption that the plasma puff contains no trapped field, the increase in flux between  $r_p$  and  $r_3$  may be equated to the decrease in flux inside the plasma. If  $\Delta\phi_p$  represents this flux change, then

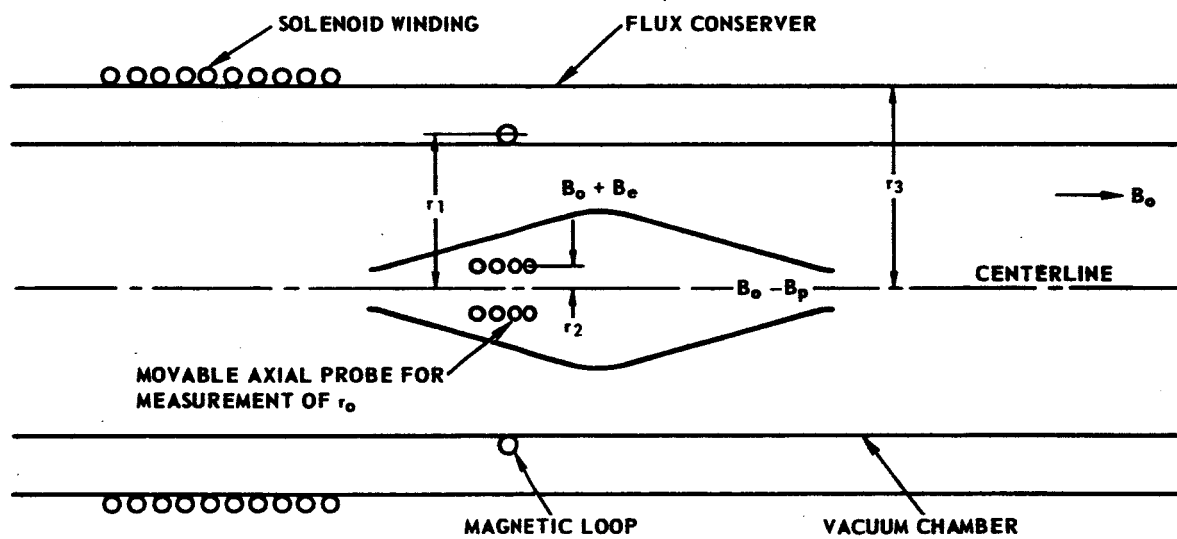


Fig. 2 Magnetic Loop and Field Geometry

$$\Delta \phi_p = 2\pi \int_0^{r_p} B_p r dr = 2\pi \int_{r_p}^{r_s} B_e r dr . \quad (43)$$

Since  $B_e$  is assumed to be uniform between  $r_p$  and  $r_s$ , Eq. 43 becomes

$$B_e = \frac{\Delta \phi_p}{\pi(r_s^2 - r_p^2)} . \quad (44)$$

The flux,  $\phi(t)$ , at any time  $t$  encircled by our magnetic loop (shown in Fig. 2) may be expressed as

$$\begin{aligned} \phi(t) &= \underbrace{\pi r_p^2 (B_o - B_p)}_{\text{flux inside plasma}} + \underbrace{\pi(r_s^2 - r_p^2) (B_o + B_e)}_{\text{flux outside plasma encircled by magnetic loop}} \\ &= -\Delta \phi_p + \pi(r_s^2 - r_p^2) B_e + \pi r_s^2 B_o \\ &= -\Delta \phi_p \left[ 1 - \frac{r_s^2 - r_p^2}{r_s^2 - r_p^2} \right] + \pi r_s^2 B_o \end{aligned} \quad (45)$$

The emf generated is then given by

$$\epsilon = -\frac{\partial \phi}{\partial t} = \left[ 1 - \frac{r_s^2 - r_p^2}{r_s^2 - r_p^2} \right] \frac{\partial \Delta \phi_p}{\partial t} - \pi r_s^2 \frac{\partial B_o}{\partial t} . \quad (46)$$

If the signal is now integrated with a passive network, the detected voltage has the form

$$v = \frac{1}{RC} \left[ 1 - \frac{r_s^2 - r_p^2}{r_s^2 - r_p^2} \right] \Delta \phi_p - \frac{\pi r_s^2 B_o}{RC} . \quad (47a)$$

In fact, the last term of this equation can be eliminated quite adequately by using a second loop far down the field, and subtracting its signal from Eq. 47a, i. e.,

$$v = \frac{1}{RC} \left[ 1 - \frac{r_1^2 - r_p^2}{r_3^2 - r_p^2} \right] \Delta \phi_p . \quad (47b)$$

Now it is necessary to relate the probe signal (Eq. 47b) to the theory of Section II. This will be done by using  $\Delta \phi_p$ .

For a straight magnetic field and hydromagnetic equilibrium (see Ref. 2)

$$p + \frac{B^2}{2\mu_0} = \text{constant} . \quad (48)$$

In the present case, this becomes

$$p + \frac{(B_o - B_p)^2}{2\mu_0} = \frac{(B_o + B_e)^2}{2\mu_0} \quad (49)$$

at the plasma-field boundary. Assuming  $B_e \ll B_o$ , Eq. 49 shows that

$$\frac{B_p}{B_o} = 1 - \sqrt{1 - \beta} = \frac{\beta}{1 + \sqrt{1 - \beta}} , \quad (50)$$

and from Eq. 43

$$\Delta \phi_p = \int_{S_p} B_p \, dS = B_o \int_{S_p} \frac{\beta}{1 + \sqrt{1 - \beta}} \, dS , \quad (51)$$

where  $S_p$  = the plasma cross-sectional area.

But  $p = W_{\perp} V$ , the transverse energy per unit volume, and thus Eq. 51 yields

$$\Delta \phi_p = \frac{2\mu_0}{B_o} \int_{S_p} \frac{W_{\perp} V \, dS}{1 + \sqrt{1 - \beta}} = \frac{2\mu_0}{B_o} \frac{W_{\perp} V}{1 + \sqrt{1 - \beta}} , \quad (52)$$

or, by using Eq. 40,

$$\begin{aligned}
 \Delta \phi_p &= B_o \int_{S_p} (1 - \sqrt{1-\beta}) dS = \pi r_p^2 B_o (1 - \sqrt{1-\beta}) \\
 &= \pi r_p^2 B_o \left[ 1 - \frac{B}{B_o} \right] \\
 &= \pi r_p^2 B_o (1 + A - \sqrt{A^2 + 1}) . \quad (53)
 \end{aligned}$$

The following expression then links the voltage (Eq. 47b) to the theory:

$$\begin{aligned}
 v &= \frac{\pi r_p^2 B_o}{RC} \left[ \frac{r_3^2 - r_1^2}{r_3^2 - r_p^2} \right] (1 + A - \sqrt{A^2 + 1}) \\
 &= \frac{\pi B_o r_o^2}{RC (\sqrt{A^2 + 1} - A)} \left[ \frac{r_3^2 - r_1^2}{r_o^2} \right] (1 + A - \sqrt{A^2 + 1}) . \quad (54)
 \end{aligned}$$

This expression gives the time behavior of the diamagnetic signal induced by the plasma at any location in space.



#### IV. DETERMINATION OF PARAMETERS FROM MAGNETIC SIGNALS

Since six parameters ( $\lambda_0$ ,  $r_0$ ,  $Z_0$ ,  $(T_e + T_i)_0$ ,  $N_1$ ,  $v_0$  or their equivalents must be determined, six relatable experimental quantities are needed. As in the French work, four magnetic loop signals are used to obtain five pieces of information:

1. Each of three loop signals gives the maximum value of the voltage,  $v_1^*$ ,  $v_2^*$ ,  $v_4^*$ .
2. The difference in the time when the maxima of loop 1 and loop 4 signals occur, i. e.,  $t_4^* - t_1^*$ , is used
3. The full width at half-maximum of the loop 3 signals, plotted as  $A_3$  vs  $t$ , which is denoted  $\Delta t \left[ \frac{A^*}{2} \right]_3$ .

where  $*$  denotes maximum of quantity and  $t^*$  denotes time at which maximum occurs.

The flux tube radius,  $r_0$ , is determined independently, giving a total of six experimental quantities. It should be pointed out that these are in no way unique, nor is there any reason to believe at present that they are the best choice (in terms of being most sensitive in fitting the data).

Determination of  $r_0$  -- There are several ways of determining  $r_0$ , such as electric probe measurements far down the flight path, time-integrated photography, and the ratio of magnetic signals from loops with different radii at the same axial position. These are well outlined in the reports listed above (see Ref. 1).

The last method has been used in the present work. An axial probe of radius  $r_2$  was inserted into the vacuum system so that the probe and one of the magnetic loops (usually number 3 or 4) were coplanar. This is

shown schematically in Fig. 2. A comparison of the signals induced by the plasma in these probes makes it possible to deduce the flux tube radius,  $r_o$ , as well as the plasma radius  $r_p$ . This method is described below:

Equation 47b gives the voltage recorded by a single-turn magnetic loop surrounding the vacuum system. When the axial probe is used, two cases are to be considered:  $r_2 > r_p$  and  $r_2 < r_p$ . Clearly, case 1 is covered by Eq. 47b where  $r_1$  is replaced by  $r_2$ . It is equally clear that the ratio of the recorded voltages yields no information about  $r_p$  (and thus about  $r_o$ ).

For case 2, however, the flux through the axial probe as a function of time is given by

$$\varphi(t) = \pi r_2^2 (B_o - B_p),$$

from which it follows that

$$v_{\text{axial}} = \frac{1}{RC} \left[ \frac{r_2}{r_p} \right]^2 \Delta \varphi_p - \frac{\pi r_2^2 B_o}{RC}. \quad (55)$$

This expression is dependent on  $r_p$ . From the ratio,  $\rho$ , of the loop voltage,  $v_{\text{loop}}$ , to the probe voltage,  $v_{\text{axial}}$ , measured at the same time, it is found that

$$r_p^2 = \frac{\rho r_2^2 r_3^2}{(r_3^2 - r_1^2 + \rho r_2^2)}, \quad (56)$$

and that

$$r_o = \left[ r_p^2 - \frac{v_{\text{loop}} RC}{\pi B_o} \left( \frac{r_3^2 - r_p^2}{r_3^2 - r_1^2} \right) \right]^{\frac{1}{2}}. \quad (57)$$

The question arises whether the axial probe disturbs the plasma markedly in this measurement. This was investigated both in the French work and in the present work. In the former investigation,  $r_0$  as measured by the above techniques was approximately 10% smaller than that found by other methods. In the present case, the magnetic loop signals were essentially unchanged by the presence of the probe; nevertheless, the four loop signals used in this analysis were recorded with this probe withdrawn and a separate run was made for the purpose of measuring  $r_0$ . (see Fig. 3).

Extraction of Data from Magnetic Loop Signals--Five quantities remain to be obtained from the magnetic loop signal: the maximum voltages from loops 1, 2, and 4 ( $v_1^*$ ,  $v_2^*$ ,  $v_4^*$ ),  $t_4^* - t_1^*$ , and the full width at half-maximum of loop 3 signal plotted  $A_3$  vs  $t$ .

The first four of these items may be read directly from oscilloscope tracings. The last quantity is slightly more cumbersome to obtain; the oscilloscope trace ( $v_3$  vs  $t$ ) must be converted into a plot of  $A_3$  vs  $t$ . Using Eqs. 40 and 54, it can be shown that

$$A = \frac{1}{2} \left[ \frac{1 - K^2}{K} \right], \quad (58)$$

where

$$K = \frac{\left[ \left( \frac{r_3}{r_0} \right)^2 - \left( \frac{r_1}{r_0} \right)^2 + \frac{v_3 RC}{\pi r_0^2 B_0} \right]}{\left[ \left( 1 + \frac{v_3 RC}{\pi r_0^2 B_0} \right) \left( \frac{r_3}{r_0} \right)^2 - \left( \frac{r_1}{r_0} \right)^2 \right]}. \quad (59)$$

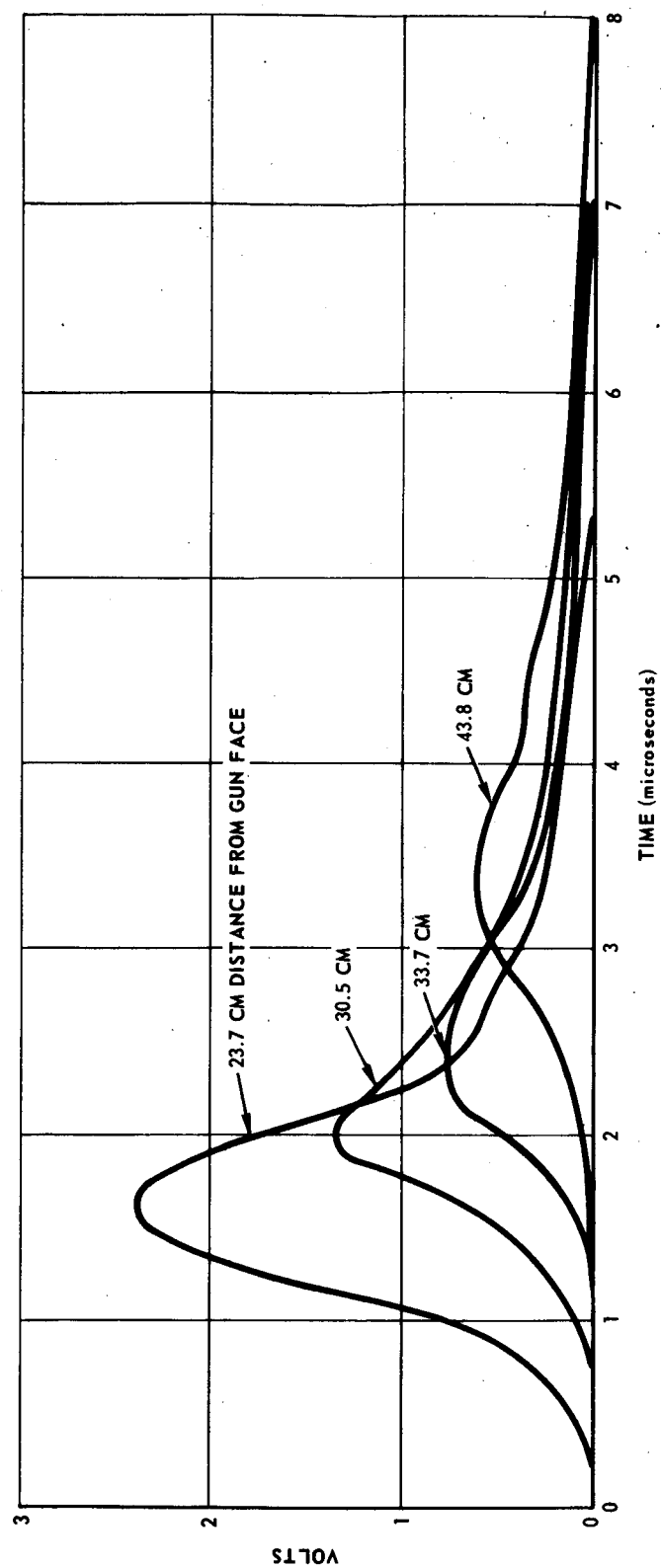


Fig. 3 Domain of Allowable Values of  $(t^*, \Delta^*)$

These equations permit the data (in the form of  $v_3$  vs  $t$ ) to be plotted as  $A_3$  vs  $t$  from which  $\Delta t \left[ \frac{A}{2} \right]_3^*$  can be determined graphically.  $A_1^*$ ,  $A_2^*$ , and  $A_4^*$  (which correspond to  $v_1^*$ ,  $v_2^*$  and  $v_4^*$ ) can also be calculated.

The correspondence is due to the fact that  $v$  is a monotonic increasing function of  $A$ .

The information necessary to carry out the analysis has now been obtained. It should be mentioned that the calculations described in this section (Eqs. 56, 57, 58, and 59) were done on a computer as was a large fraction of the work to be discussed in the following section. These computer programs are described in the appendices.

## V. ANALYSIS

The analysis is carried out essentially by graphical methods, in which successive approximations are used to give the best fit to the data.

The analysis procedure will be outlined first and is based on the assumption that the necessary graphs are available. Then the means of obtaining these curves will be discussed. The required graphs are as follows:

1. The family of curves  $f^*(\alpha, Z') = \text{constant}$  where  $f^*(\alpha, Z')$  is the maximum of the function (Eq. 35) with respect to  $\tau$ .
2. The family of curves  $\tau^* = \text{constant}$  as a function of  $(\alpha, Z')$  where  $\tau^*$  is the reduced time at which the maximum of  $f(\Lambda, \alpha, Z')$  occurs, independent of the value of  $f^*$  for the particular  $(\alpha, Z', \Lambda)$ .
3. The family of curves  $\Delta \tau_{\frac{1}{2}} = \text{constant}$  as a function of  $\alpha, Z'$ , where  $\Delta \tau_{\frac{1}{2}}$  is the full width at half-maximum of the function  $f(\alpha, Z', \Lambda)$ , plotted as a function of  $\tau$ .

The following ratios are constructed next:

$$Q_{12} = \frac{Z_2' - Z_1'}{Z_4' - Z_1'} = \frac{Z_2 - Z_1}{Z_4 - Z_1}, \quad (60a)$$

$$Q_{13} = \frac{Z_3 - Z_1}{Z_4 - Z_1} = \frac{Z_3 - Z_1}{Z_4 - Z_1}, \quad (60b)$$

$$K_2 = \frac{f^*(\alpha, Z_2')}{f^*(\alpha, Z_1')} = \frac{A_2^*}{A_1^*}, \quad (60c)$$

and

$$K_4 = \frac{f^*(\alpha, Z_4')}{f^*(\alpha, Z_1')} = \frac{A_4^*}{A_1^*} \quad (60d)$$

The equality of the ratios can be seen from Eqs. 30 and 37.

It is noteworthy that the first terms to the right of the equal signs are constructed of variables from the theory while the second terms are made up of experimental determinable quantities. (The values  $A_1^*$  are calculated from the values of  $v_1^*$ ;  $Z_1$  is the distance from the center of the gun coil to the loop positions). These are experimental values for the ratios in Eq. 60 for which a best fit in the  $(\alpha, Z^1)$  plane must be found.

A starting set  $(\alpha, Z_1^1)$  is chosen arbitrarily. The corresponding  $f^*(\alpha, Z_1^1)$  is found from the graphs of  $f^* = \text{constant}$ . Then a value of

$$f^*(\alpha, Z_4^1) = K_4^{\text{exp}} f^*(\alpha, Z_1^1)$$

is calculated. (Superscript "exp" indicates experimentally determined values.) With this value of  $f^*(\alpha, Z_4^1)$  the coordinate  $Z_4^1$  which corresponds to the value  $[ \alpha, f^*(\alpha, Z_4^1) ]$  is located on the graph. Since from Eq. 60a  $Z_2^1 = Z_1^1 + Q_{12}(Z_4^1 - Z_1^1)$ , it is possible to find  $f^*(\alpha, Z_2^1)$  at the coordinates  $(\alpha, Z_2^1)$  and construct

$$K_2 = \frac{f^*(\alpha, Z_2^1)}{f^*(\alpha, Z_1^1)}$$

based on an estimate of  $(\alpha, Z_1^1)$  and compare it to  $K_2^{\text{exp}}$  derived from the data. This procedure is repeated and the choice of  $(\alpha, Z_1^1)$  is adjusted until good agreement is achieved between  $K_2$  and  $K_2^{\text{exp}}$ . In this manner the range of  $(\alpha, Z_1^1)$  is limited.

These values of  $(\alpha, Z_1^1)$  are used with the second set of graphs,  $\tau^* = \text{constant}$  as a function of  $(\alpha, Z^1)$ . The experimental information to be used is the difference in the times at which the maxima  $v_4^*$  and  $v_1^*$  occur, i. e.,  $t_4^* - t_1^*$ . From Eq. 21b

$$\xi = \frac{t_4^* - t_1^*}{\tau_4^* - \tau_1^*} \quad (61)$$

Locating  $\tau_4^*$  at  $(\alpha, Z_4')$  and  $\tau_1^*$  at  $(\alpha, Z_1')$ ,  $\xi$  may be evaluated.

It is now possible to limit further the allowable values of  $(\alpha, Z_1')$  by using the full width at half-maximum of the signal from loop 3.  $\Delta \tau_{\frac{1}{2}}$  at  $(\alpha, Z_3')$  may be found from the curves  $\Delta \tau_{\frac{1}{2}} = \text{constant}$ , where Eq. 60b becomes

$$Z_3' = Z_1' + Q_{13} (Z_4' - Z_1')$$

For the proper values of  $(\alpha, Z_1')$

$$\left[ \Delta \tau_{\frac{1}{2}} \right]_3 = \frac{1}{\xi} \Delta t \left[ \frac{A}{2} \right]_3^* \quad (62)$$

Generally it is necessary to repeat these three steps several times in order to achieve the best fit to the data. This sequential processing permits one to limit to a fairly narrow domain the allowable range into which the characterizing parameters fall. (Waelbroeck et al, Ref. 1, find acceptable fits with  $\lambda \pm 8\%$ ,  $N_i \pm 6\%$ ,  $Z_0 \pm 1.5 \text{ cm}$ ,  $(T_e + T_i)_0 \pm 15\%$ ,  $v_0 \pm 5\%$ ).

As a final step these parameters are used to calculate the voltages from Eq. 54 and compare them to the traces recorded by the oscilloscope.



## VI. COMPUTER ANALYSIS

The computer analysis to be described below was carried out on the IBM 7094 computer at APL/JHU. It is by no means the most sophisticated means of conducting the analysis but is designed to eliminate some of the mathematical drudgery which the method described in Section V requires.

The programming is divided into five parts:

1. The calculations of  $r_p$ ,  $r_o$ ,  $A_3$  vs  $t$ ,  $A_1^*$ ,  $A_2^*$ ,  $A_4^*$  and the ratios  $K_2$ ,  $K_4$ ,  $Q_{12}$ ,  $Q_{13}$ , (Subsec. V).
2. The calculation of the family of curves  $f^*(\alpha, Z') = \text{constant}$ .
3. The calculation of the family of curves  $\tau^*(\alpha, Z') = \text{constant}$ .
4. The calculation of the family of curves  $\Delta\tau_{\frac{1}{2}}(\alpha, Z') = \text{constant}$ .
5. The calculation of the voltages using the parameters from the analysis, the local velocity and the volume density  $n_i$ .

Each of these calculations will be treated in turn.

The Fortran listings of these programs are given in Appendix V.

Reduction of Magnetic Loop Data-- This program is the most straightforward of the five. The mathematics is outlined in Subsec. .IV and needs little further explanation. In this program, the Mks system of units is used and the indicated times are in microseconds.

The input data necessary to this program are:

1.  $V_{loop}$ ; VOUT (the peak voltage from the magnetic loop for measurement of  $r_0$ )
2.  $V_{axial}$ ; VIN (the peak voltage from the axial probe for measurements of  $r_0$ )
3.  $r_2$ ;  $R_2$  (radius of the axial probe;  $\sqrt{n} r_2$  is used for more than one turn)
4.  $R$ ,  $R'$ ;  $R$ , RPR (the resistance in integrator from the loop and the axial probe, respectively)
5.  $C$ ,  $C'$ ;  $C$ , CPR (the capacitance in integrator from the loop and the axial probe, respectively)
6.  $r_3$ ;  $R_3$  (flux conserver radius)
7.  $r_1$ ;  $R_1$  (magnetic loop radius)
8.  $v_1^*$ ,  $v_2^*$ ,  $v_3^*$ ,  $v_4^*$ ; VMAX 1 (voltage maxima from loops)
9.  $t_1^*$ ,  $t_2^*$ ,  $t_3^*$ ,  $t_4^*$ ; TMAX 1 (time at which the voltage maxima occur)
10.  $Z_1$ ,  $Z_2$ ,  $Z_3$ ,  $Z_4$ ;  $Z_1$  (location of loops from the center of the gun coil)
11.  $B_0$ ;  $B_0$  (magnetic field intensity of drift field)
12.  $v_3$  vs  $t$  (loop 3 voltage and the corresponding times)

The output data are shown in the appendix for a typical case. They are:

- (1)  $r_0$ , (2)  $r_p$ , (3)  $A_1^*$ ,  $A_2^*$ ,  $A_3^*$ ,  $A_4^*$ , (4)  $A_3$  vs  $t$ , (5)  $K_2$ ,  $K_4$ ,  $Q_{12}$ ,  $Q_{13}$

Calculation of Curves  $f^*(\alpha, Z') = \text{Constant}$ -- The equal-value curves of  $f^*(\alpha, Z')$  are obtained in the following way:

$$f(\Lambda, \alpha, Z') = \Lambda^{-5/3} \exp - \left[ \frac{Z' - \alpha\tau}{\Lambda} \right]^2 \quad (\text{Eq. 35}).$$

In order to find the maximum of  $f$  with respect to  $\tau$ ,  $\frac{df}{d\tau}$  is set equal to zero yielding

$$2 \left[ \frac{Z' - \alpha\tau}{\Lambda} \right]^2 \frac{d\Lambda}{d\tau} + 2\alpha \left[ \frac{Z' - \alpha\tau}{\Lambda} \right] - \frac{5}{3} \frac{d\Lambda}{d\tau} = 0 \quad (63)$$

Solving Eq. 63 as a quadratic in  $\left[ \frac{Z' - \alpha\tau}{\Lambda} \right]$ , and requiring that this argument remain finite as  $\alpha \rightarrow \infty$ , i. e.,  $[(T_e + T_i)_0 \rightarrow 0]$  gives

$$\frac{Z' - \alpha\tau^*}{\Lambda^*} = \frac{-\alpha + \sqrt{\alpha^2 + \frac{10}{3} (1 - \Lambda^{*-2/3})}}{2 [1 - \Lambda^{*-2/3}]^{1/2}} \quad (\text{at maximum}), \quad (64)$$

$$\text{where } \frac{d\Lambda}{d\tau} = [1 - \Lambda^{-2/3}]^{1/2} \quad (\text{Eq. 24}).$$

Eq. 35 may be written in the form

$$- \left[ \frac{Z' - \alpha\tau}{\Lambda} \right] = \ln f + \frac{5}{3} \ln \Lambda \quad (65)$$

Equations 64 and 65, at the maximum, are combined to give

$$\alpha = \frac{\left[ \frac{5}{6} + \ln f^* + \frac{5}{3} \ln \Lambda^* \right] [1 - \Lambda^{*-2/3}]}{\sqrt{-\ln f^* - \frac{5}{3} \ln \Lambda^*}} \quad (66)$$

The curves  $f^*(\alpha, Z') = \text{constant}$  may be found using this expression.

First the constant, which may range between 0 and 1 is chosen; then a set of values of  $\alpha$  are generated (using Eq. 66) for a series of values  $\Lambda^*$  greater than 1. The corresponding  $Z'$  is then calculated from Eq. 64 and the expression  $\tau(\Lambda)$  is given by

$$\tau^* = \left[ \Lambda^{*2/3} + 2 \right] \left[ \Lambda^{*2/3} - 1 \right]^{\frac{1}{2}} \quad (\text{Eq. 23}).$$

The restrictions on the allowable values for the pairs  $(f^*, \Lambda^*)$  are readily found from Eq. 66 to be

$$e^{-5/6} \leq f^* \Lambda^{*5/3} < 1. \quad (67)$$

This domain is shown graphically in Fig. 4.

Since the equal-value curves,  $f^*(\alpha, Z') = \text{constant}$  and  $\tau^*(\alpha, Z') = \text{constant}$ , were computed in the same program, discussion of this program's input-output data will be deferred until the end of the next subsection.

Calculation of the Curves  $\tau^*(\alpha, Z') = \text{Constant}$ -- This calculation is conducted in a manner similar to that of the preceding section. First, a value  $\Lambda^* = \text{constant}$  is chosen and this implies a value for  $\tau^* = \text{constant}$  (Eq. 23); a series of values of  $\alpha$  are then introduced into Eq. 64 to find  $Z'$ . Thus the sets  $(\alpha, Z')$  for which  $\tau^* = \text{constant}$  are generated and this process is repeated for successive values of  $\Lambda^*$ .

There are two parts to the input data to this program: input data for  $f^*(\alpha, Z') = \text{constant}$  and input data for  $\tau^*(\alpha, Z') = \text{constant}$ .

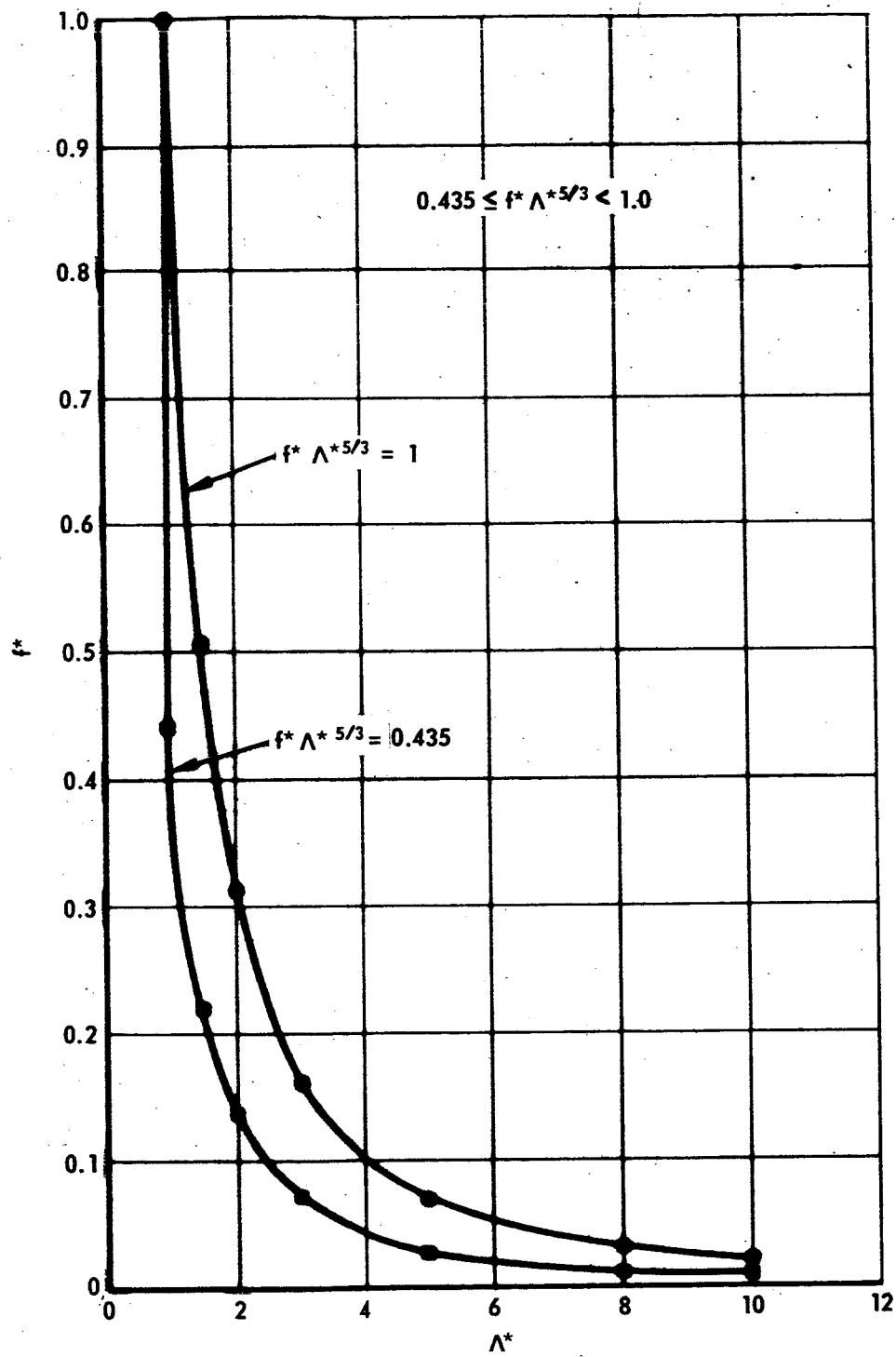


Fig. 4 Typical Magnetic Loop Signals

A. The input data for  $f^*(\alpha, Z')$  are:

1. Initial value of  $f^*$  : FMAX
2. Initial value of  $\Lambda^*$  : XLAM
3. Incremental change in  $f^*$ ,  $(\Delta f^*)$  : DELFMX
4. Incremental change in  $\Lambda^*$ ,  $(\Delta \Lambda^*)$  : DELAM
5. M, the number of values of  $f^*$  to be used.
6. N, the number of values of  $\Lambda^*$  to be used.

B. The input data for  $\tau^*(\alpha, Z') = \text{constant}$  are:

1. Initial value of  $\alpha$  : XALPA
2. Initial values of  $\Lambda^*$  : YLAM
3. Incremental change in  $\alpha$ ,  $(\Delta \alpha)$  : DELALP
4. Incremental change in  $\Lambda^*$ ,  $(\Delta \Lambda^*)$  : DEYLAM
5. L, the number of values of  $\Lambda^*$  to be used.
6. K, the number of values of  $\alpha$  to be used.

Similarly, the output data are divided into two parts.

A. The output data for  $f^*(\alpha, Z')$  are:

1. The value of  $f^*$
2. A listing of  $\alpha, Z', \tau^*, \Lambda^*$  corresponding to this value of  $f^*$

B. The output data for  $\tau^*(\alpha, Z') = \text{constant}$  are:

1. The value of  $\tau^*$
2. A listing of  $\alpha$  and  $Z'$  corresponding to this value of  $\tau^*$

For the purposes of the analysis these data were graphed. Typical curves are shown in Figs. 3 and 5.

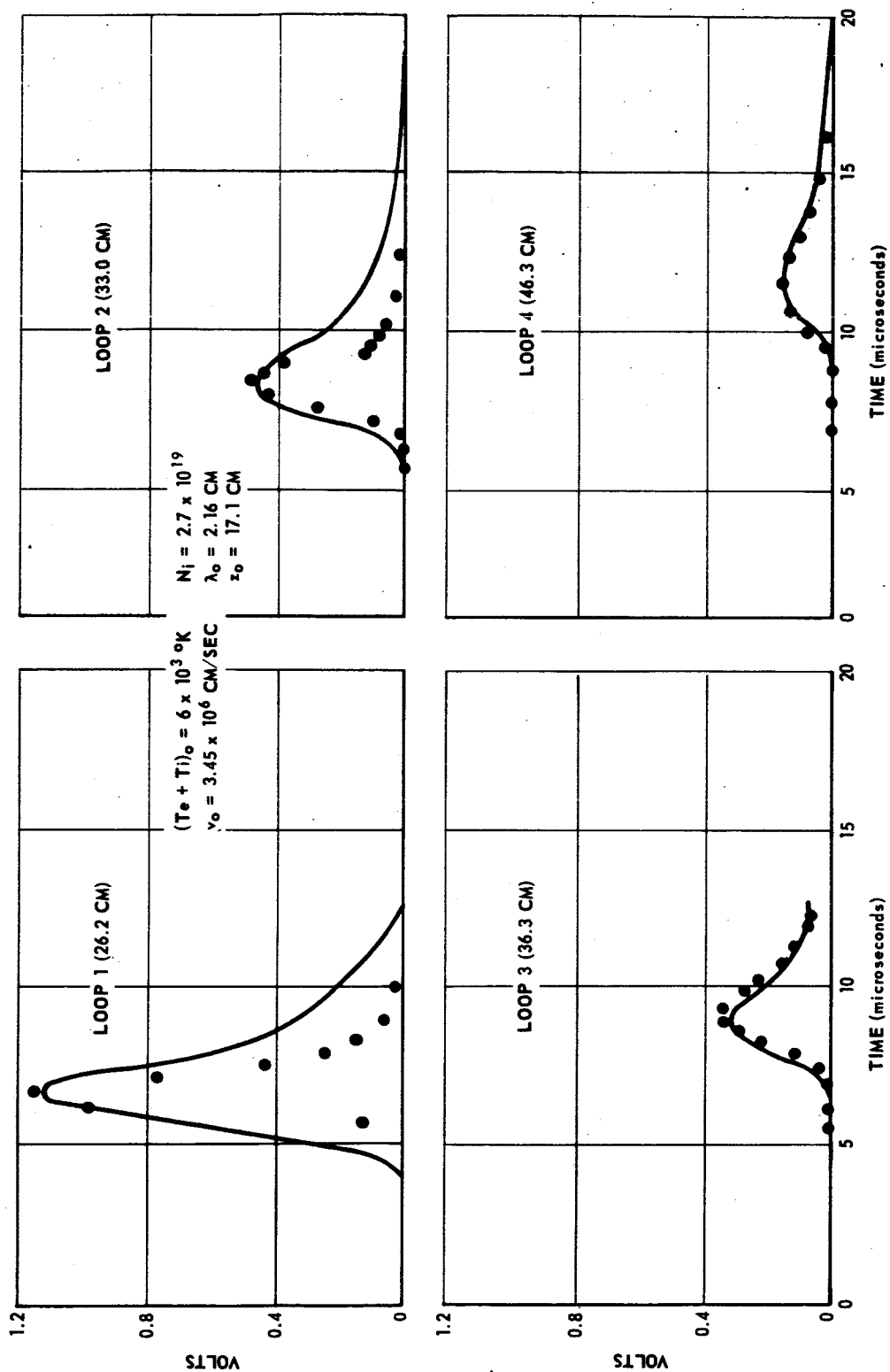


Fig. 5 Comparison of Magnetic Loop Signals with Analysis (points), Condition I

Calculation of the Curves  $\Delta\tau_{\frac{1}{2}} = \text{Constant}$ -- This is by far the most complicated calculations and probably the most interesting from the programmer's point of view.

The full width at half-maximum,  $\Delta\tau_{\frac{1}{2}}$ , is given by

$$\Delta\tau_{\frac{1}{2}} = \tau_2 - \tau_1, \quad (68)$$

where  $\tau_2$  and  $\tau_1$  are the reduced times at which the function  $f(\Lambda, \alpha, Z')$  achieves half-maximum values,  $\frac{1}{2}f^*$ . The widths are found in the following way: A value of  $\Lambda^*$  (and thus  $\tau^*$ ), and a value of  $\alpha$  are chosen;  $Z'$  is calculated from Eq. 64. Next  $f(\Lambda^*, \alpha, Z') \equiv f^*$  is computed. Finally the roots of the following equations are found:

$$\frac{1}{2}f^* = \Lambda_1^{-5/3} \exp - \left[ \frac{Z' - \alpha\tau_1}{\Lambda_1} \right]^2, \quad (69a)$$

with

$$1 < \Lambda_1 \leq \Lambda^*,$$

and

$$\frac{1}{2}f^* = \Lambda_2^{-5/3} \exp - \left[ \frac{Z' - \alpha\tau_2}{\Lambda_2} \right]^2, \quad (69b)$$

with

$$\Lambda^* \leq \Lambda_2 \leq M\Lambda^*,$$

where  $M$  is some sufficiently large multiplier. Having found  $\Lambda_1$  and  $\Lambda_2$ ,  $\tau_1$ ,  $\tau_2$ , and  $\Delta\tau_{\frac{1}{2}}$  are found directly. In the present case, a bisectional method was used to find the roots  $\Lambda_1$  and  $\Lambda_2$  of Eqs. 69a and 69b to an accuracy of 0.001. (For this purpose,  $\tau_1$  and  $\tau_2$  were expressed in terms of  $\Lambda_1$  and  $\Lambda_2$  according to Eq. 24.



For each value of  $\Lambda^*$ , a list of  $\alpha$ ,  $Z'$  and  $\Delta\tau_{\frac{1}{2}}$  is calculated. The values of  $\alpha$  used in this program were the same for each  $\Lambda^*$  ( $\Lambda^*$  ranged from 1 to 10).

The graphs  $\Delta\tau_{\frac{1}{2}}(\alpha, Z') = \text{constant}$  are obtained by first plotting the family of curves  $\alpha = \text{constant}$  as a function of  $\Delta\tau_{\frac{1}{2}}$  and  $Z'$ , and then interpolating to find the curves desired. These curves are presented in Fig. 6.

The input data for this program consist of:

1. The accuracy to which the roots  $\Lambda_1$  and  $\Lambda_2$  are to be found: EPS
2. The initial value of  $\alpha$ : XALFA
3. Initial values of  $\Lambda^*$ : XLAM
4. Incremental change in  $\alpha$ ,  $(\Delta\alpha)$ : DEALF
5. Incremental change in  $\Lambda^*$ ,  $(\Delta\Lambda^*)$ : DEXLM
6. M, the number of values of  $\Lambda^*$  to be used.
7. N, the number of values of  $\alpha$  to be used.

The output data for this program consist of:

1.  $\Lambda^*$ : LAMAX
2.  $\alpha$ : ALPHA
3.  $Z'$ : ZPRME
4.  $\Delta\tau_{\frac{1}{2}}$ : WIDTH
5. Calculated value of  $\frac{1}{2}f^*$  at root  $\Lambda_1$ : F1
6. Calculated value of  $\frac{1}{2}f^*$  at root  $\Lambda_2$ : F2
7.  $\Lambda_1$  near root found by the program: XLAM1
8.  $\Lambda_2$  for root found by the program: XLAM2
9.  $f^*$ : FMAX

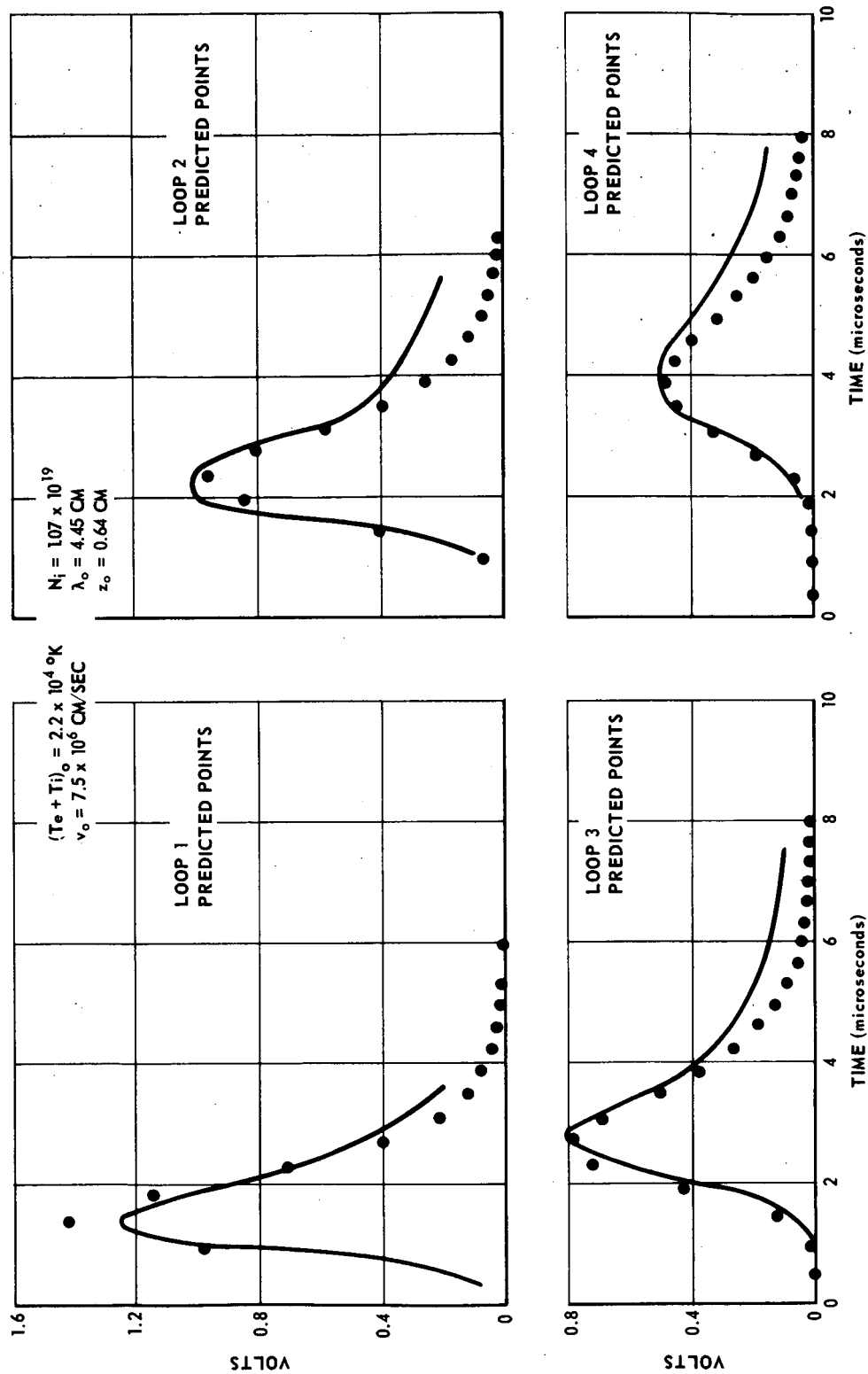


Fig. 6 Comparison of Magnetic Loop Signals with Analysis (points), Condition II

Reconstruction of Magnetic Signals--When the curves described above are available, the analysis of Section V can be carried out to find the five remaining unknown parameters which describe the plasma. The final step is to reconstruct the four magnetic-loop signals based on the theory and using the extracted parameters.

The parameters which are found from the analysis are  $\lambda_0$ ,  $\alpha$ ,  $\xi$ ,  $r_0$ ,  $N_i$ , and  $Z_0$ . The loop signals are reconstructed by substituting the above data in Eq. 37 to find  $A$  as a function of  $t$ , by first calculating  $A(\Lambda)$  and then converting  $\Lambda$  to the time domain. Using these results,  $v$  as a function of time is then calculated from Eq. 54.

In the program used here, the volume density,  $n_i(Z, t)$  and the local velocity,  $v(Z, t)$ , were also calculated.

The input data for this program consist of:

1. Value of  $\alpha$  : ALPHA
2. Initial value of  $\Lambda$  : XLAM
3. Incremental steps in  $\Lambda$  : DX
4. Value of  $\lambda_0$  : XLAMO
5. Value of  $Z_0$  : ZO
6.  $N$ , the number of steps in  $\Lambda$  to be made
7. Value of  $r_0$  : RO
8. Value of  $r_1$  : R1
9. Value of  $r_3$  : R3
10. Value of  $B_0$  : BO
11. Integrator time constant, RC: RC
12. Center-of-mass velocity,  $v_1$  : VO
13. Ion mass,  $m_i$  : XM

14. Total number of ions,  $N_i$ : XN
15. Value of  $\xi$ : XI
16. Loop location, Z, and the last loop location: Z, ZLAST.

The output data are:

1. The characteristic parameters
2. The voltage V, the time t, A,  $\tau$ ,  $\Lambda$ , density  $n_i$ , and velocity v.

A separate listing is given for each loop location, Z.

This now makes the calculated signals available to be compared to the oscilloscope traces.

## VII. RESULTS

The analyses of two plasma puffs are presented here. The initial conditions in the two cases were significantly different, these differences being reflected in the final plasma characteristics.

Figure 4 shows a typical set of magnetic loop signals to which the foregoing analysis was applied. The positions of the loops relative to the gun face are indicated.

Figure 5 shows the fit obtained for one case. The solid curves represent the loop signals while the points indicate the values computed by the theoretical method. This plasma can be characterized as dense and cool. As can be seen from the figure, the fit improves as the plasma advances through the drift field. The plasma characteristics arrived at are:

$$(T_e + T_i)_0 = 6 \times 10^3 \text{ }^\circ\text{K}$$

$$v_0 = 3.45 \times 10^6 \text{ cm/sec}$$

$$N_i = 2.7 \times 10^{19} \text{ ions}$$

$$\lambda_0 = 2.16 \text{ cm}$$

and

$$Z_0 = 17.1 \text{ cm}$$

Of some concern is the fact that the computed curve decays more rapidly than the signal itself. No satisfactory explanation for this has been found. A possible explanation may be that the field from the gun influences the magnitude of the first loop signal significantly, in which case the value of  $A_1^*$  is different from the value which would be obtained otherwise. The resulting "best" set of parameters to fit the data, especially for a low-temperature plasma, are adversely affected.

The low temperature and high density calculated for this case suggest the possibility that the assumptions for the computation may not be fulfilled. Initial trapped field, recombination, or diffusion may be playing a role. Further experimental measurements are expected to clarify this picture.

Figure 6 shows the fit to the second plasma puff. The fit to these data clearly is considerably better. This plasma has the following characteristics:

$$\begin{aligned}(T_e + T_i)_0 &= 2.2 \times 10^4 \text{ }^\circ\text{K} \\ v_0 &= 7.5 \times 10^6 \text{ cm/sec} \\ N_i &= 1.07 \times 10^{19} \text{ ions} \\ \lambda_0 &= 4.45 \text{ cm} \\ Z_0 &= 0.64 \text{ cm}\end{aligned}$$

The fit to all four signals is quite good, with a marked improvement in the fit to the trailing edge of the pulses. In support of the previous discussion, it can be seen that better overall fits were obtained by sacrificing the fit to the magnitude of the first signal.

It should be noted that the  $\beta$  calculated for this case comes out to 0.86, which though physically reasonable and not in disagreement with the observed puff size, does cast some doubt on the numbers above.

## VIII. DISCUSSION

Further analysis of the plasmas derived from the gun is planned, both with the longitudinal field and the magnetic octupole field using this model.

The shifting of the pick-up loops downstream will be attempted to establish whether the gun influences the signal from the first loop sufficiently to affect the final results.

It is noteworthy that although the gun and the drift field used here were quite similar to the arrangement used by the French investigators, the plasmas produced here are typically denser and of lower temperature than those produced by the prototype gun. It is quite likely that these discrepancies are due to the difference in gun frequency (the present gun has a ring frequency of 80 kc while the French gun's frequency was a factor of two higher).

## APPENDIX I

### Solution of Equation 10b

The following relationship was found:

$$n_i V = - \lambda' \int \left[ \frac{2Z^2}{\lambda^3} n_i - \frac{n_i}{\lambda} \right] dZ, \quad (10b)$$

or

$$n_i V = - \frac{\lambda' N_A}{\sqrt{\pi}} \int \left[ \frac{2Z^2}{\lambda^4} \exp - \left( \frac{Z}{\lambda} \right)^2 - \frac{1}{\lambda^2} \exp - \left( \frac{Z}{\lambda} \right)^2 \right] dZ.$$

Let

$$Z^2 = x, \quad \text{then } dz = \frac{dx}{2\sqrt{x}}.$$

Thus,

$$n_i V = - \frac{\lambda' N_A}{\sqrt{\pi}} \int \left[ \frac{\sqrt{x}}{\lambda^4} \exp - \left( \frac{x}{\lambda^2} \right) - \frac{1}{2\lambda^2} \exp - \left( \frac{x}{\lambda^2} \right) \right] dx. \quad (10c)$$

Integrating the first term on the right yields

$$\int \frac{\sqrt{x}}{\lambda^4} \exp - \left[ \frac{x}{\lambda^2} \right] dx = - \frac{\sqrt{x}}{\lambda^2} \exp - \left[ \frac{x}{\lambda^2} \right] + \frac{1}{2\lambda^2} \int \frac{1}{\sqrt{x}} \exp - \left[ \frac{x}{\lambda^2} \right] dx + c,$$

where C is the constant of integration.



Equation 10c now becomes

$$n_i V = \frac{\lambda' N_A}{\lambda' \sqrt{\pi}} Z \exp - \left[ \frac{Z}{\lambda} \right]^2 + c. \quad (10d)$$

Since  $V$  is the velocity relative to the center of mass of the plasma puff, the velocity of the particles at a distance  $+z$  must be equal to the velocity of particles at  $-z$ . Thus, the constant  $C$  must be identically zero.

$$V = \frac{Z \lambda'}{\lambda} \quad \text{Q. E. D.} \quad (11)$$

## APPENDIX II

### Solution of Equation 12

$$\frac{\partial p}{\partial Z} + \frac{n_i m_i Z \lambda''}{\lambda} = 0$$

$$p = - \int \frac{n_i m_i Z \lambda''}{\lambda} dZ = - \frac{N_A \lambda''}{\sqrt{\pi}} m_i \int \frac{Z}{\lambda^2} \exp - \left[ \frac{Z}{\lambda} \right]^2 dZ .$$

It should be noted that taking  $N_A$  outside the integral sign is again invoking the assumption that  $r_p$  is a slowly varying function  $z$ .

Again letting  $Z^2 = x$ ,

$$p = - \frac{N_A \lambda''}{\sqrt{\pi}} m_i \int \frac{1}{2\lambda^2} \exp - \left[ \frac{x}{\lambda^2} \right] dx ,$$

$$p = \frac{m_i N_A}{2 \sqrt{\pi}} \lambda'' \exp - \left[ \frac{Z}{\lambda} \right]^2 + c ,$$

as  $Z \rightarrow \pm \infty$ ,  $p \rightarrow 0$ .

Thus,

$$p = \frac{m_i N_A}{2 \sqrt{\pi}} \lambda'' \exp - \left[ \frac{Z}{\lambda} \right]^2 .$$

Using Eq. 8, we have

$$p = \frac{1}{2} n_i m_i \lambda \lambda'' \quad \text{Q. E. D.}$$

### APPENDIX III

#### Solution of Equation 22

$$3 \Lambda \frac{d^2 \Lambda}{d\tau^2} + \left[ \frac{d\Lambda}{d\tau} \right]^2 = 1. \quad (22)$$

Let  $p = \frac{d\Lambda}{d\tau},$

Then  $\frac{dp}{d\tau} = \frac{d^2 \Lambda}{d\tau^2} = \frac{dp}{d\Lambda} \frac{d\Lambda}{d\tau};$

$$\therefore \frac{d^2 \Lambda}{d\tau^2} = p' p,$$

where

$$p' = \frac{dp}{d\Lambda}.$$

Equation 22 now may be rewritten as follows:

$$3 p' p \Lambda + p^2 = 1. \quad (22a)$$

Multiplying both sides of Eq. 22a by  $\Lambda^{n-1}$  yields

$$3 \Lambda^n p' p + p^2 \Lambda^{n-1} = \Lambda^{n-1}. \quad (22b)$$

But  $\frac{d}{d\Lambda} (C p^2 \Lambda^n) = 2 C p p' \Lambda^n + n C p^2 \Lambda^{n-1},$

where  $C$  is some constant. This expression is exactly equal to the left side of Eq. 22b if

$$2C = 3 \quad \text{and} \quad nC = 1 ;$$

$$C = 3/2 \quad n = 2/3 .$$

Equation 22b may be written as

$$\frac{d}{d\Lambda} (3/2 p^2 \Lambda^{2/3}) = \Lambda^{-1/3} .$$

Integration of this equation gives

$$3/2 p^2 \Lambda^{2/3} = 3/2 \Lambda^{2/3} + L ,$$

or

$$p^2 = 1 + M \Lambda^{-2/3} ,$$

where  $M$  is the constant of the integration.

$$p = \frac{d\Lambda}{d\tau} = (1 + M \Lambda^{-2/3})^{\frac{1}{2}}$$

$$d\tau = \frac{d\Lambda}{(1 + M \Lambda^{-2/3})^{\frac{1}{2}}}$$

Let  $y^3 = \Lambda .$

Then  $d\Lambda = 3y^2 dy ,$

and 
$$d\tau = \frac{3y^2 dy}{(1 + My^{-2})^{\frac{1}{2}}} = \frac{3y^3 dy}{(y^2 + M)^{\frac{1}{2}}} ,$$

$$\tau = (y^2 - 2M)(y^2 + M)^{\frac{1}{2}} ,$$

$$\tau = (\Lambda^{2/3} - 2M)(\Lambda^{2/3} + M)^{\frac{1}{2}} , \quad (22c)$$

$$\text{at } t = \tau = 0 \quad \Lambda = 1.$$

$$\therefore M = -1 \text{ or } 1/2.$$

Using Eq. 22c, Eq. 25 of the text becomes

$$\frac{(T_e + T_i)}{(T_e + T_i)_0} = - \frac{M}{\Lambda^{2/3}},$$

and since ratio must be positive,  $M = -1$ .

Thus we find

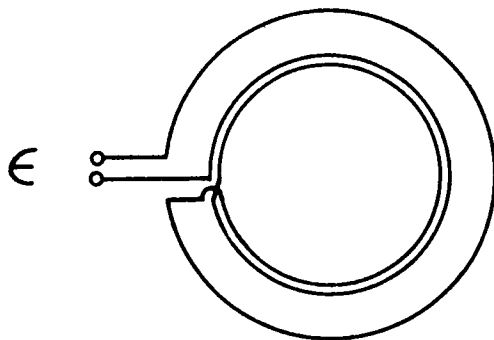
$$\tau = (\Lambda^{2/3} + 2)(\Lambda^{2/3} - 1)^{1/2}, \quad (23)$$

$$\frac{d\Lambda}{d\tau} = (1 - \Lambda^{-2/3})^{1/2}. \quad \text{Q. E. D.} \quad (24)$$

## APPENDIX IV

### The Compensated Magnetic Loops

The compensated loops used by the French investigators effectively consisted of two loops of equal areas in opposition. One of these loops encircles the plasma while the other encloses an area outside the plasma but inside the flux conserver. (see sketch below)



Schematic of Compensated Magnetic Loop Arrangement

The flux passing through the loop may be calculated by means of

$$\phi(t) = \pi r_p^2 (B_o - B_p) + \pi (r_i^2 - r_p^2) (B_o + B_e) - \pi r_i^2 (B_e + B_o)$$

where  $B_o$  = field intensity from solenoid

$B_p$  = field generated internal to plasma

and

$B_e$  = field due to flux excluded by plasma

The first term above represents the flux through the plasma cross section. The second term is the flux in the region between the plasma and

the loop which encircles the plasma, while the last term is the flux encircled by the compensating element whose effective area is equal  $\pi r_1^2$ .

$$\therefore \phi(t) = -\pi r_p^2 B_p - \pi r_p^2 B_e$$

But

$$\pi r_p^2 B_p = \Delta \phi_p = \pi (r_s^2 - r_p^2) B_e$$

and thus

$$\phi(t) = -\Delta \phi_p \left[ 1 + \frac{r_p^2}{r_s^2 - r_p^2} \right]$$

The e.m.f.,  $\epsilon$ , is given by

$$\epsilon = -\frac{\partial \phi}{\partial t} = \left[ 1 + \frac{r_p^2}{r_s^2 - r_p^2} \right] \frac{\partial \Delta \phi_p}{\partial t}$$

and the integrated signal

$$v = \frac{1}{RC} \left[ 1 + \frac{r_p^2}{r_s^2 - r_p^2} \right] \Delta \phi_p$$

This type of magnetic loop has the obvious advantage of eliminating the effect of the  $B_o$  field.

## APPENDIX V

### Computer Listings



# REDUCTION OF SINGLE LOOP DATA'RO CALCULATION

```

DIMENSION V3(56),T3(56),A3X(56),D3X(56)
DXXF(S,T,U,X,Y) = (((S/T)**2.)-(U/T)**2.)+(X/Y)/((1.+(X/Y))*((S
1/T)**2.)-(U/T)**2.))
AXXF(X) = (1.-(X**2.))/(2.*X)
55 READ INPUT TAPE 5,300,VOUT,VIN,R2,RPR,CPR
READ INPUT TAPE 5,300,R3,R1,B0,R,C
READ INPUT TAPE 5,305,VMAX1,VMAX2,VMAX3,VMAX4
READ INPUT TAPE 5,305,TMAX1,TMAX2,TMAX3,TMAX4
READ INPUT TAPE 5,305,Z1,Z2,Z3,Z4
PI= 3.1415927
RATIO=VOUT/VIN
RPSQ=(R3**2.)*(R2**2.)*(RATIO*R*C)/((RPR*CPR)*((R3**2.)-(R1**2.)+(
1R2**2.)*((RATIO*R*C)/(RPR*CPR))))
RO=SQRTF(RPSQ-(((R*C*VOUT)*((R3**2.)-(RPSQ)))/(PI*B0*((R3**2.)-(R1
1**2.)))))
RP=SQRTF(RPSQ)
BETA=1.0-((RO/RP)**4.)
WRITE OUTPUT TAPE 6,308,RO,RP,B0,BETA
XK=(PI*(RO**2.)*B0)/(R*C)
DMX1= DXXF(R3,RO,R1,VMAX1,XK)
DMX2= DXXF(R3,RO,R1,VMAX2,XK)
DMX3= DXXF(R3,RO,R1,VMAX3,XK)
DMX4= DXXF(R3,RO,R1,VMAX4,XK)
AMAX1= AXXF(DMX1)
AMAX2= AXXF(DMX2)
AMAX3= AXXF(DMX3)
AMAX4= AXXF(DMX4)
WRITE OUTPUT TAPE 6,301,AMAX1,AMAX2,AMAX3,AMAX4,VMAX1,VMAX2,VMAX3,
1VMAX4,TMAX1,TMAX2,TMAX3,TMAX4
READ INPUT TAPE 5,302,N
READ INPUT TAPE 5,303,(V3(I),I=1,N)
READ INPUT TAPE 5,303,(T3(I),I=1,N)
WRITE OUTPUT TAPE 6,304
DO 5 I=1,N
D3X(I)=DXXF(R3,RO,R1,V3(I),XK)
5 A3X(I)=AXXF(D3X(I))
WRITE OUTPUT TAPE 6,306,(I,A3X(I),T3(I),V3(I),I=1,N)
Q12 =(Z2-Z1)/(Z4-Z1)
Q13 =(Z3-Z1)/(Z4-Z1)
YK2 = (AMAX2)/(AMAX1)
YK4 = (AMAX4)/(AMAX1)
WRITE OUTPUT TAPE 6,307,Q12,Q13,YK2,YK4
GO TO 55
300 FORMAT (5F10.6)
301 FORMAT (7X,6HAMAX1=F7.3,3X,6HAMAX2=F7.3,3X,6HAMAX3=F7.3,3X,6HA
1MAX4=F7.3/(7X,6HVMAX1=F7.3,3X,6HVMAX2=F7.3,3X,6HVMAX3=F7.3,3X,6HVM
2AX4=F7.3)/(7X,6HTMAX1=F7.3,3X,6HTMAX2=F7.3,3X,6HTMAX3=F7.3,3X,6HTM
3AX4=F7.3))
302 FORMAT (5X,I2)
303 FORMAT(7F10.6)
304 FORMAT (2X,1H1,7X,2HA3,8X,2HT3,8X,2HV3,/)
305 FORMAT (4F10.6)
306 FORMAT (1X,I2,3X,F8.3,2X,F8.3,2X,F8.3)
307 FORMAT (7X,4HQ12=F7.3,3X,4HQ13=F7.3/(7X,3HK2=F7.3,3X,3HK4=F7.3))
308 FORMAT(1H1,6X,3HRO=F10.6,6HMETERS,3X,3HRP=F10.6,6HMETERS,3X,3HB0=F

```

REDUCTION OF SINGLE LOOP DATA'RO CALCULATION

110.6,4HW/M2,3X,5HBETA=F10.6)

END(1,1,0,0,0,0,1,1,0,0,0,0,0,0,0)

CALCULATION OF  $\tau^*$  = CONSTANT

MOSS

```

      XEQ
      DIMENSION XLAMX(51),TAUMXM(50),ALPHA(50,50),ZPRME(50,50),FMAXM(51)
      1,YLAMX(51),TAUX(51),ALPA(51),ZPRMX(50,50)
      ALFAF(X,Y)=(((5./6.)+(LOGF(X)+(5./3.)*LOGF(Y)))*SQRTF(1.-Y**(-2./3
      1.)))/(SQRTF(-(LOGF(X))-(5./3.)*LOGF(Y)))
      TAUMXF(X)= (X**((2./3.)+2.)*SQRTF(X**((2./3.)-1.))
      ZPRMF(X,Y,Z)=X*Z-(X*Y-Y*SQRTF(X**2.+(10./3.)*(1.-Y**(-2./3.))))/(2
      1.*SQRTF(1.-Y**(-2./3.)))
11  READ INPUT TAPE 5,100,FMAX,XLAM,DELFMX,DELAM,M,N
      FMAXM(1)=FMAX
      XLAMX(1)=XLAM
      DO 20 I=1,M
      WRITE OUTPUT TAPE 6,101,I,FMAXM(I),DELFMX,DELAM
      DO 30 J=1,N
      TAUMXM(J)=TAUMXF(XLAMX(J))
      ALPHA(I,J)=ALFAF(FMAXM(I),XLAMX(J))
      ZPRME(I,J)=ZPRMF(ALPHA(I,J),XLAMX(J),TAUMXM(J))
      XLAMX(J+1)=XLAMX(J)+DELAM
30  CONTINUE
      WRITE OUTPUT TAPE 6,102,(J,ALPHA(I,J),ZPRME(I,J),TAUMXM(J),XLAMX(J
      1),J=1,N)
      FMAXM(I+1)=FMAXM(I)+DELFMX
20  CONTINUE
      READ INPUT TAPE 5,100,XALPA,YLAM,DELALP,DEYLAM,L,K
      ALPA(1)=XALPA
      YLAMX(1)=YLAM
      DO 50 I=1,L
      TAUX(I)=TAUMXF(YLAMX(I))
      WRITE OUTPUT TAPE 6,203
      WRITE OUTPUT TAPE 6,201,I,TAUX(I),YLAMX(I),DELALP,DEYLAM
      DO 60 J=1,K
      ZPRMX(I,J)=ZPRMF(ALPA(J),YLAMX(I),TAUX(I))
      ALPA(J+1)=ALPA(J)+DELALP
60  CONTINUE
      WRITE OUTPUT TAPE 6,202,(J,ALPA(J),ZPRMX(I,J),J=1,K)
      YLAMX(I+1)=YLAMX(I)+DEYLAM
50  CONTINUE
      GO TO 11
100 FORMAT (4F10.6,2I6)
101 FORMAT (1H1,5X,2HI=I3,5X,6HFMAXM=F7.3,5X,7HDELFMX=F7.3,5X,6HDELAM=
      1F7.3//(2X,1HJ,5X,5HALPHA,9X,5HZPRME,9X,6HTAUMXM,8X,5HLAMAX))
102 FORMAT(1X,I2,3X,F9.5,5X,F10.5,5X,F9.4,5X,F9.4)
201 FORMAT      (5X,2HI=I3,5X,7HTAUMAX=F7.3,5X,6HLAMAX=F7.3,5X,9HDELALP
      1HA=F7.3,5X,6HDELAM=F7.3//(2X,1HJ,5X,5HALPHA,9X,5HZPRME))
202 FORMAT (1X,I2,3X,F9.5,5X,F10.5)
203  FORMAT(1H1,25X,30HCALCULATION OF TAUMAX=CONSTANT/(26X,29HAS A FUNC
      ITION OF ALPHA,ZPRIME))
      END(1,1,0,0,0,0,1,1,0,0,0,0,0,0,0)

```

```

DIMENSION ALPA(51),YLAMX(51),TAUX(51),ZPRME(50,50),CHECK(51,51),FM
1AX(51,51),M(51,51)
ZPRME(X,Y,Z)=X*Z-(X*Y-Y*SQRTF(X**2.+(10./3.)*(1.-Y**(-2./3.))))/(2
1.*SQRTF(1.-Y**(-2./3.)))
TAUMXF(X)=(X**(.2/3.)+2.)*SQRTF(X**(.2/3.)-1.)
FCTF(W,X,Y,Z)=(W**(-5./3.))*EXP(-((Z-X*Y)/W)**2.)
11 READ INPUT TAPE 5,100,XALPA,YLAM,DELALP,DEYLAM,L,K
Y=EXP(-5./6.)
ALPA(1)=XALPA
YLAMX(1)=YLAM
DO 50 I=1,L
TAUX(I)=TAUMXF(YLAMX(I))
WRITE OUTPUT TAPE 6,203
WRITE OUTPUT TAPE 6,201,I,TAUX(I),YLAMX(I),DELALP,DEYLAM
DO 60 J=1,K
ZPRME(I,J)=ZPRME(ALPA(J),YLAMX(I),TAUX(I))
FMAX(I,J)=FCTF(YLAMX(I),ALPA(J),TAUX(I),ZPRME(I,J))
CHECK(I,J)=FMAX(I,J)*(YLAMX(I)**(5./3.))
IF(CHECK(I,J)-1.) 51,51,52
51 IF(CHECK(I,J)-Y) 52,53,53
52 M(I,J)=0
GO TO 60
53 M(I,J)=1
60 ALPA(J+1)=ALPA(J)+DELALP
WRITE OUTPUT TAPE 6,202, (J,ALPA(J),ZPRME(I,J),FMAX(I,J),CHECK(I,J
1),M(I,J),J=1,K)
50 YLAMX(I+1)=YLAMX(I)+DEYLAM
GO TO 11
100 FORMAT(4F10.6,2I6)
203 FORMAT(1H1,25X,30HCALCULATION OF TAUMAX=CONSTANT/(26X,29HAS A FUNC
1TION OF ALPHA,ZPRIME))
201 FORMAT(5X,2HI=I3,5X,7HTAUMAX=F7.3,5X,6HLAMAX=F7.3,5X,9HDELALPHA=F7
1.3,5X,6HDELAM=F7.3/(2X,1HJ,5X,5HALPHA,10X,5HZPRME,8X,4HFMAX,8X,5H
2CHECK,8X,4HTEST))
202 FORMAT(1X,I2,3X,F9.5,5X,F10.5,5X,F9.5,3X,F9.5,6X,I1)
END(1,1,0,0,0,0,1,1,0,0,0,0,0,0,0)

```

# CALCULATION OF $\Delta T$

```

DIMENSION ZPRME(5,5),ALPHA(5),XLAMX(5),XLAM1(5,5),XLAM2(5,5),TAUX(
15),T1(5,5),T2(5,5),FMAX(5,5),WIDTH(5,5),RESULT(5),FX2(5,5),FX1(5,5
2)
COMMON ZPRME,ALPHA,F12,I,J
FXXF(W,X,Y,Z)=(X**(-5./3.))*EXPF(-(((Z-W*Y)/X)**2.))
ZPRMF(X,Y,Z)=X*Z-(X*Y-Y*SQRTF(X**2.+(10./3.)*(1.-Y**(-2./3.))))/(2
1.*SQRTF(1.-Y**(-2./3.)))
TAUF(X)=(X**(2./3.)+2.)*SQRTF(X**(2./3.)-1.)
25 READ INPUT TAPE 5,602,EPS
READ INPUT TAPE 5,600,XALFA,XLAM,DEALF,DEXLM,M,N
ALPHA(1)=XALFA
XLAMX(1)=XLAM
DO 90 I=1,M
WRITE OUTPUT TAPE 6,601,I,XLAMX(I)
TAUX(I)=TAUF(XLAMX(I))
DO 91 J=1,N
ZPRME(I,J)= ZPRMF(ALPHA(J),XLAMX(I),TAUX(I))
FMAX(I,J) = FXXF(ALPHA(J),XLAMX(I),TAUX(I),ZPRME(I,J))
F12=0.5*FMAX(I,J)
DUMMY
XL1=1.00001
XLM=XLAMX(I)
XL2 =(5.0)*XLAMX(I)
CALL BROUT(XLM,XL2,RESULT,EPS,DUMMY)
IF(RESULT(2)-XLM) 50,51,50
51 IF(RESULT(3)-XL2) 50,52,50
52 WRITE OUTPUT TAPE 6,604
GO TO 91
50 XLAM2(I,J)=RESULT(1)
CALL BROUT(XL1,XLM,RESULT,EPS,DUMMY)
IF(RESULT(2)-XL1) 40,41,40
41 IF(RESULT(3)-XLM) 40,42,40
42 WRITE OUTPUT TAPE 6,604
GO TO 91
40 XLAM1(I,J)=RESULT(1)
T1(I,J)=TAUF(XLAM1(I,J))
T2(I,J)=TAUF(XLAM2(I,J))
WIDTH(I,J)= T2(I,J)-T1(I,J)
CHECK= FMAX(I,J)*(XLAMX(I)**(5./3.))
Y=EXPF(-5./6.)
IF (Y-CHECK) 20,20,21
21 WRITE OUTPUT TAPE 6,603,CHECK
GO TO 91
20 IF (CHECK-1.) 30,30,21
30 FX1(I,J)=FXXF(ALPHA(J),XLAM1(I,J),T1(I,J),ZPRME(I,J))
FX2(I,J)=FXXF(ALPHA(J),XLAM2(I,J),T2(I,J),ZPRME(I,J))
WRITE OUTPUT TAPE 6,605,J,ALPHA(J),ZPRME(I,J),WIDTH(I,J),FX1(I,J),
1FX2(I,J),XLAM1(I,J),XLAM2(I,J),FMAX(I,J)
91 ALPHA(J+1)=ALPHA(J)+DEALF
90 XLAMX(I+1)=XLAMX(I)+DEXLM
GO TO 25
600 FORMAT (4F10.6,2I5)
601 FORMAT(1H1,5X,2HI=I2,5X,6HXLAMX=F10.6,/,/(2X,1HJ,5X,5HALPHA,10X,5H
1ZPRME,9X,5HWIDTH,10X,2HF1,10X,2HF2,9X,5HXLAM1,9X,5HXLAM2,9X,4HFMAX
2))
602 FORMAT (F10.6)
603 FORMAT(1X,46HCHECK DOES NOT MEET PHYSICAL CRITERION CHECK=F10.6)
604 FORMAT (31HNO ROUT OR EVEN NUMBER OF ROOTS)
605 FORMAT(1X,I2,4X,F10.6,5X,F10.6,4X,F10.6,5X,F9.6,3X,F9.6,3X,F10.6,4

```

1X,F10.6,4X,F10.6)  
END

# BISECTIONAL ROOT FINDER FOR $\Delta T$ PROGRAM

```

SUBROUTINE BROJT (X1,X2,RESULT,EPS,DUMMY)
DIMENSION ZPRMC(5,5),ALPHA(5),XLAMX(5),XLAM1(5,5),XLAM2(5,5),TAUX(
15),T1(5,5),T2(5,5),FMAX(5,5),WIDTH(5,5),RESULT(5),FX2(5,5),FX1(5,5
2)
TX1=X1
TX2=X2
F1=DUMMY(TX1)
F2=DUMMY(TX2)
Q=2.*EPS
IF(F1)1,2,2
1 IF(F2)9,3,3
2 IF(F2)3,9,9
3 U=.5*(TX1+TX2)
F3=DUMMY(U)
IF(F3)4,5,5
4 IF(F1)7,6,6
5 IF(F1)6,7,7
6 F2=F3
TX2=U
GO TO 8
7 F1=F3
TX1=U
8 IF(ABSF(TX2-TX1)-Q)9,3,3
9 RESULT(1)=.5*(TX1+TX2)
RESULT(2)=TX1
RESULT(3)=TX2
RESULT(4)=F1
RESULT(5)=F2
RETURN
END

```

MCSS

```
FUNCTION DUMMY(X)
  DIMENSION ZPRME(5,5),ALPHA(5),XLAMX(5),XLAM1(5,5),XLAM2(5,5),TAUX(
15),T1(5,5),T2(5,5),FMAX(5,5),WIDTH(5,5),RESULT(5),FX2(5,5),FX1(5,5
2)
  COMMON ZPRME,ALPHA,F12,I,J
  DUMMY=F12*(X**(5./3.))-EXP(-(((ZPRME(I,J)-ALPHA(J))*((X**(2./3.))+
12.)*SQRT(((X**(2./3.))-1.)))/X)**2.))
  RETURN
END(1,1,0,0,0,0,1,1,0,0,0,0,0,0,0)
```



# RECONSTRUCTION OF VOLTAGE TRACES

MOSS

```

DIMENSION A(50),Y(50),XLAX(51),F(50),TAUX(50),V(50),T(50),DENS(50)
1,VEL(50)
FCTF(W,X,Y,Z)=(W**(-5./3.))*EXP(-((Z-X*Y)/W)**2.)
TAUF(X)=((X**(2./3.))+2.)*SQRTF((X**(2./3.))-1.)
92 READ INPUT TAPE 5,900,ALPHA,XLAM,DX,XLAMO,ZO,N
READ INPUT TAPE 5,901,R0,R1,R3,B0,RC
READ INPUT TAPE 5,902,V0,XM,XN,XI
PI=3.1415927
XMU= PI*4.0E-07
C= (XMU*XN*XM*V0)/(6.0*(PI**(3./2.))*ALPHA*XI*(R0**2.)*(B0**2.))
91 READ INPUT TAPE 5,903,Z,ZLAST
ZPRME =(Z-ZO)/(XLAMO)
XLAX(1)=XLAM
DO 90 I=1,N
TAUX(I)=TAUF(XLAX(I))
F(I)=FCTF(XLAX(I),ALPHA,TAUX(I),ZPRME)
A(I)=C*F(I)
Y(I)= SQRTF((A(I)**2.)+1.)-A(I)
V(I)= ((PI*B0)/RC)*(1.-Y(I))*((R0**2.)/Y(I))*(((R3**2.)-(R1**2.))/
1((R3**2.)-(R0**2.)/Y(I)))
DENS(I)= ((XN/((PI**(3./2.))*XLAMO*(R0**2.)))*Y(I)*EXP(-((ZPRME-A
1LPHA*TAUX(I))/XLAX(I))**2.))/XLAX(I)
VEL(I)=(XLAMO/XI)*(ALPHA+((ZPRME-ALPHA*TAUX(I))/XLAX(I))*SQRTF(1.-
1(XLAX(I)**(-2./3.))))
T(I)=XI*TAUX(I)
90 XLAX(I+1)=XLAX(I)+DX
WRITE OUTPUT TAPE 6,904,Z,ALPHA,XM,XN,ZO,V0,XLAMO,B0,XI
WRITE OUTPUT TAPE 6,906
WRITE OUTPUT TAPE 6,905,(I,V(I),T(I),A(I),TAUX(I),XLAX(I),DENS(I),
1VEL(I),I=1,N)
IF(Z-ZLAST) 91,92,92
900 FORMAT (5F10.6,I5)
901 FURMAT (4F10.6,E10.4)
902 FORMAT (4E10.4)
903 FORMAT (2F10.6)
904 FORMAT(1H1,5X,2HZ=F5.3,7H METERS,3X,6HALPHA=F6.3,3X,5HMASS=E10.3,6
1H KGRMS,3X,5HIONS=E10.3/(6X,3HZO=F5.3,7H METERS,3X,3HVO=E10.2,6H M
2/SEC,3X,6HXLAMO=F5.3,7H METERS,3X,3HB0=F7.4,5H W/M2,3X,3HXI=E10.3,
34H SEC,/)
905 FORMAT(2X,I2,3X,F6.3,3X,E10.3,4X,F7.3,4X,F7.3,4X,F7.4,3X,E10.3,4X,
1E10.3)
906 FORMAT(3X,1H1,6X,1HV,11X,1HT,11X,1HA,9X,3HTAU,5X,6HLAMBDA,7X,4HDEN
1S,9X,3HVEL)
END(1,1,0,0,0,0,1,1,0,0,0,0,0,0,0)

```

## REFERENCES

1. F. Waelbroeck, J. P. Poffe, C. Leloup, and J. Jacquinet, Report EUR-CEA-FC, Papers 112 (July 1961), 217 (May 1964), and 218 (July 1963).
2. L. Spitzer, Physics of Fully Ionized Gases, Interscience Publishers, New York and London.

# INITIAL DISTRIBUTION EXTERNAL TO THE APPLIED PHYSICS LABORATORY\*

The work reported in TG-806 was done under Bureau of Naval Weapons Contract NOw 62-0604-c  
(Task Z16) supported by BuWeps and NASA.

ORGANIZATION	LOCATION	ATTENTION	No. of Copies
DEPARTMENT OF DEFENSE			
DDC	Alexandria, Va.		20
<u>Department of the Navy</u>			
BUWEPS	Washington, D. C.	DLI-31	2
BuWepsRep	Silver Spring, Md.		1
NRL	Washington, D. C.	A. C. Kolb	1
U. S. GOVERNMENT AGENCIES			
<u>Atomic Energy Commission</u>			
Headquarters	Washington, D. C.	W. C. Gough	1
		A. E. Ruark	1
Documentation Center	Larchmont, N. Y.	Depository Library	1
Oak Ridge National Lab.	Oak Ridge, Tenn.	R. Dandl	1
Los Alamos Scientific Lab.	Los Alamos, N. M.	J. E. Phillips	1
<u>National Aero. and Space Admin.</u>			
Headquarters	Washington, D. C.	K. Thom	1

\*Initial distribution of this document within the Applied Physics Laboratory has been made in accordance with a list on file in the APL Technical Reports Group.

UNCLASSIFIED

Security Classification

## DOCUMENT CONTROL DATA - R&amp;D

(Security classification of title, body of abstract and indexing annotation must be entered when the overall report is classified)

1. ORIGINATING ACTIVITY (Corporate author) The Johns Hopkins Univ., Applied Physics Lab. 8621 Georgia Avenue Silver Spring, Maryland		2a. REPORT SECURITY CLASSIFICATION Unclassified	
		2b. GROUP	
3. REPORT TITLE EVOLUTION OF A PLASMA PUFF IN A LONGITUDINAL MAGNETIC FIELD			
4. DESCRIPTIVE NOTES (Type of report and inclusive dates) None			
5. AUTHOR(S) (Last name, first name, initial) Moss, Samuel J.			
6. REPORT DATE January 1966	7a. TOTAL NO. OF PAGES	7b. NO. OF REFS	
8a. CONTRACT OR GRANT NO. NOW 62-0604-c b. PROJECT NO. c. Task Assignment Z16 d.	9a. ORIGINATOR'S REPORT NUMBER(S) TG-806		
	9b. OTHER REPORT NO(S) (Any other numbers that may be assigned this report) None		
10. AVAILABILITY/LIMITATION NOTICES Distribution of this document is unlimited.			
11. SUPPLEMENTARY NOTES None		12. SPONSORING MILITARY ACTIVITY Bureau of Naval Weapons (Department of the Navy) and NASA	
13. ABSTRACT The hydromagnetic model of the evolution of a plasma puff in a $B_z$ field described by Waelbroeck et al <sup>1</sup> has been used to analyze the characteristics of the plasma produced by the APL conical pinch gun. The analysis is based on fitting the signals induced in single turn magnetic pick-up loops by the passing plasma. In the cases studied good fits to the signals have been achieved and the characteristic parameters of the plasma found ( $n_{ion} \sim 10^{22}$ ions/m <sup>3</sup> Tion $\sim 4 \times 10^4$ °K). This analysis applied to plasma generated by the APL theta-pinch gun (A Theta-Pinch Plasma Gun by R. Turner) has not been successful. In the two cases studied, the lack of good fits is attributed to the presence of a sizeable amount of trapped field in the puff which is present along the entire flight path through the $B_z$ field.			
<sup>1</sup> F. Waelbroeck, J. P. Poffe, C. Leloup, and J. Jacquinet, EUR-CEA-FC 112, 217, 218			

14. KEY WORDS	LINK A		LINK B		LINK C	
	ROLE	WT	ROLE	WT	ROLE	WT
Plasma Gun Magnetic Field Magnetic Loop Analysis Velocity Temperature Density						

#### INSTRUCTIONS

**1. ORIGINATING ACTIVITY:** Enter the name and address of the contractor, subcontractor, grantee, Department of Defense activity or other organization (*corporate author*) issuing the report.

**2a. REPORT SECURITY CLASSIFICATION:** Enter the overall security classification of the report. Indicate whether "Restricted Data" is included. Marking is to be in accordance with appropriate security regulations.

**2b. GROUP:** Automatic downgrading is specified in DoD Directive 5200.10 and Armed Forces Industrial Manual. Enter the group number. Also, when applicable, show that optional markings have been used for Group 3 and Group 4 as authorized.

**3. REPORT TITLE:** Enter the complete report title in all capital letters. Titles in all cases should be unclassified. If a meaningful title cannot be selected without classification, show title classification in all capitals in parenthesis immediately following the title.

**4. DESCRIPTIVE NOTES:** If appropriate, enter the type of report, e.g., interim, progress, summary, annual, or final. Give the inclusive dates when a specific reporting period is covered.

**5. AUTHOR(S):** Enter the name(s) of author(s) as shown on or in the report. Enter last name, first name, middle initial. If military, show rank and branch of service. The name of the principal author is an absolute minimum requirement.

**6. REPORT DATE:** Enter the date of the report as day, month, year, or month, year. If more than one date appears on the report, use date of publication.

**7a. TOTAL NUMBER OF PAGES:** The total page count should follow normal pagination procedures, i.e., enter the number of pages containing information.

**7b. NUMBER OF REFERENCES:** Enter the total number of references cited in the report.

**8a. CONTRACT OR GRANT NUMBER:** If appropriate, enter the applicable number of the contract or grant under which the report was written.

**8b, 8c, & 8d. PROJECT NUMBER:** Enter the appropriate military department identification, such as project number, subproject number, system numbers, task number, etc.

**9a. ORIGINATOR'S REPORT NUMBER(S):** Enter the official report number by which the document will be identified and controlled by the originating activity. This number must be unique to this report.

**9b. OTHER REPORT NUMBER(S):** If the report has been assigned any other report numbers (*either by the originator or by the sponsor*), also enter this number(s).

**10. AVAILABILITY/LIMITATION NOTICES:** Enter any limitations on further dissemination of the report, other than those

imposed by security classification, using standard statements such as:

- (1) "Qualified requesters may obtain copies of this report from DDC."
- (2) "Foreign announcement and dissemination of this report by DDC is not authorized."
- (3) "U. S. Government agencies may obtain copies of this report directly from DDC. Other qualified DDC users shall request through \_\_\_\_\_."
- (4) "U. S. military agencies may obtain copies of this report directly from DDC. Other qualified users shall request through \_\_\_\_\_."
- (5) "All distribution of this report is controlled. Qualified DDC users shall request through \_\_\_\_\_."

If the report has been furnished to the Office of Technical Services, Department of Commerce, for sale to the public, indicate this fact and enter the price, if known.

**11. SUPPLEMENTARY NOTES:** Use for additional explanatory notes.

**12. SPONSORING MILITARY ACTIVITY:** Enter the name of the departmental project office or laboratory sponsoring (*paying for*) the research and development. Include address.

**13. ABSTRACT:** Enter an abstract giving a brief and factual summary of the document indicative of the report, even though it may also appear elsewhere in the body of the technical report. If additional space is required, a continuation sheet shall be attached.

It is highly desirable that the abstract of classified reports be unclassified. Each paragraph of the abstract shall end with an indication of the military security classification of the information in the paragraph, represented as (TS), (S), (C), or (U).

There is no limitation on the length of the abstract. However, the suggested length is from 150 to 225 words.

**14. KEY WORDS:** Key words are technically meaningful terms or short phrases that characterize a report and may be used as index entries for cataloging the report. Key words must be selected so that no security classification is required. Identifiers, such as equipment model designation, trade name, military project code name, geographic location, may be used as key words but will be followed by an indication of technical context. The assignment of links, rules, and weights is optional.